

Chapter 6

Nanoparticle-Based Diamond Electrodes

Geoffrey W. Nelson and John S. Foord

Abstract This chapter reviews the construction, modification, and physical characteristics of two types of diamond electrodes: nanoparticle-modified diamond electrodes (NMDE) and detonation nanodiamond-based electrodes (DNDE). These particular types of diamond electrodes show great promise for improving the performance of diamond electrodes via the incorporation of nano-scale chemistry at their surfaces. The construction of both types of electrodes are reviewed, along with the resultant physical and electronic effects. The methods reviewed here are particularly applicable for electroanalytic and electrocatalytic applications of nanoparticle-based diamond electrodes. A brief review of progress on the interactions between metals and diamond at nanoparticle-based electrodes is also included. Finally, an outline of the present state-of-the art research in this field is presented.

6.1 Introduction

Carbon based materials have the potential to be an important class of materials for 21st century technologies. One particular carbon-based material has rather extreme properties—diamond. For several decades now, researchers have been excited by its transparency, extreme hardness, high thermal conductivity, bio-compatibility, and chemical resistance [1]. Examples of its utility abound. For instance, diamond is made conductive when doped, thus creating a useful electronic material. In this form, diamond can be used in biosensors, electroanalytical devices, and as a catalytic support in fuel cells [1–4]. At the cutting-edge of diamond research are efforts to investigate how nitrogen vacancies in diamond could be crucial to a functioning quantum computing device [5, 6]. The present interest in diamond remains high, as exemplified by the many reviews that describe the historical development, properties, and synthesis of this unique functional material [1, 7–12].

G.W. Nelson · J.S. Foord (✉)
Department of Chemistry, Oxford University, Oxford OX1 3TA, UK
e-mail: john.foord@chem.ox.ac.uk

There exist many types of diamond, both natural and synthetic. However, it is the conductive forms of diamond which shows the most promise as a functional material. Conductive diamond is counter-intuitive, as diamond is usually considered an insulator. However, when doped to a 1:1,000 ratio of an intentionally added impurity (e.g. B or N), diamond can become a wide band-gap semiconductor [1]. In 1986, Fujimori et al. [13] were the first to develop a polycrystalline conductive diamond film using chemical vapour deposition (CVD) and boron-doping. Since then, boron-doped diamond (BDD) has become a commercially important material (i.e. Element Six, U.K.) and is heavily used for electrochemical applications.

The p-type semiconducting properties of BDD have desirable electrochemical properties, such as its low signal to background current ratio, wide potential window, robust nature, chemical resistance, and bio-compatibility [1]. BDD also does not suffer from extensive surface corrosion, oxide formation, or have unwanted electrical interactions with deposited catalyst, thus making it a useful substrate for fundamental chemical studies of electrocatalysis [10]. Its most unfavourable trait is its relative lack of electroactivity, compared to other carbon-based materials [14]. This is due to a reduced surface concentration of the following: sp^2 carbon, delocalised electrons, and oxygenated species. These characteristics reduce its electroactivity towards several chemical reactions of industrial and biological importance, such as the methanol oxidation reaction (MOR), oxygen reduction reaction (ORR), and neurotransmitter redox reactions. Thus, to make a practical diamond-based device, some modification of the diamond surface or structure is needed.

Many of the physical, wet chemical, and electrochemical routes leading to improved electrical properties are well-reviewed by others [4, 11, 14–16]. Of the many possible modifications, the incorporation of nano-scale chemistry to the surfaces and structure of diamond is of tremendous recent interest. The two most interesting research pathways are the nanoparticle modification of diamond, and the use of unmodified or modified diamond nanoparticles. An example of each type of substrate and their modification is shown in Figs. 6.1 and 6.2.

Diamond could be modified by a film of metal or metal oxide, but this is an expensive process. It is also a process which does not benefit from the well-known catalytic properties of nano-particulate metals and metal oxides. For instance, bulk gold is relatively inert, but in nanoparticle form it is highly catalytic towards certain redox reactions, such as the ORR [17]. The properties of BDE make it an effective and stable support for these NPs. The modification of BDE with metal and metal oxide NPs has been recently reviewed by Toghiani and Compton [14]. In their review, they detail how BDE electrochemistry is enhanced by the high surface area, improved reactivity, and zero-overlap of diffusion zones, thereby ensuring maximum mass transfer of analytes or molecules to the surface [14]. The adsorption of reactants is different at nano-sized particles, compared to their macro-sized counterparts [18]. Also, the exploitation of quantum effects to enhance electrochemical reactions is possible on nanoparticles-based electrodes [18]. Consensus suggests that sub-monolayer coverage of nano-sized metals or metal oxides are effective catalysts for energy conversion and fuel cell applications.

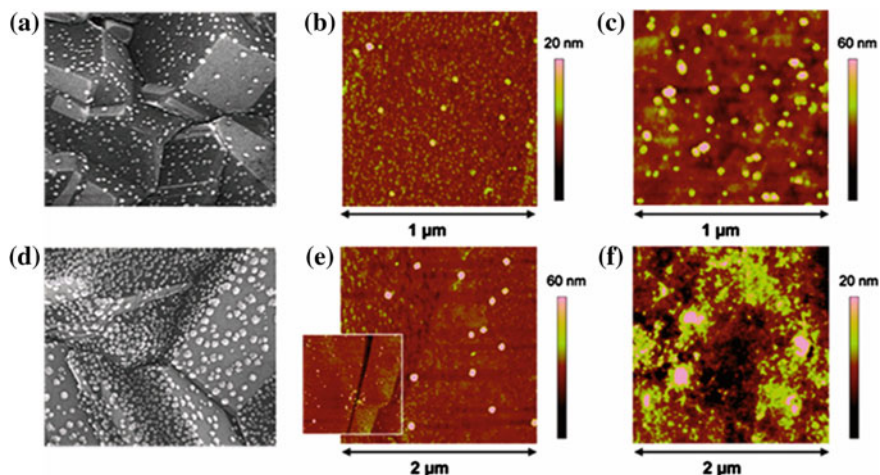


Fig. 6.1 SEM and AFM images of nanoparticles on boron-doped electrodes: SEM of BDD electrodes with Au nanoparticles after potentiostatic deposition at -0.4 V for **a** 10 s and **d** 60 s. AFM (tapping mode) of boron-doped diamond electrodes with $\text{Ni}(\text{OH})_2$ after potentiostatic deposition in which $\text{Ni}(\text{OH})_2$ was electro-precipitated onto polycrystalline boron-doped diamond electrode for **b** 1 s, **c** 15 s, **e** 30 s, and **f** 100 s. SEM images from Yamada et al. [218], with permission from Elsevier (Copyright © 2008); AFM images reprinted with permission from [56], Copyright (2011) American Chemical Society

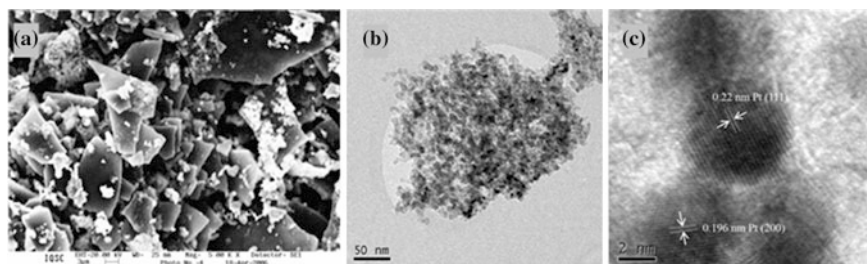


Fig. 6.2 Images of detonation nanodiamond particles decorated with nanoparticles: **a** SEM image of detonation nanodiamond powder surface decorated with Pt-RuO_x deposited by the sol-gel method; TEM **(b)** and HRTEM **(c)** images of DND powder decorated with Pt via microwave-heating of ethylene glycol solutions containing H_2PtCl_6 and the detonation nanodiamond particles. Figure adapted from Giancarlo et al. [67], with permission from Elsevier (Copyright © 2006) and from Bian et al. [150], with permission from the International Journal of Electrochemical Science (Copyright © 2012)

Alternatively, diamond can be made nano-sized via detonation of explosives in oxygen-rich environments. Unlike its bulk counterpart, detonation nanodiamond (DND) is electroactive in its undoped form. This remarkable property is due its “giant” surface area, coupled with a surface chemistry rich in reactive oxygen species, sp^2 carbon, unsaturated carbon bonds, and delocalised electrons [19]. The redox

behaviour of ND has been found to be “molecule-like”, with the reduction and oxidation of the surface occurring at discrete electrochemical potentials [19]. This relatively novel material is now used in advanced sensor and catalytical technologies. Further information can be found in reviews by Holt [5] and others [20].

While there exist reviews on the topics of nanoparticle-modified diamond electrodes (NMDE) [14] and DND-based electrodes (DNDE) [5, 11, 20], there are no reviews detailing the progress made for their construction. If one wishes to optimize the effects of nano-scale chemistry at diamond-based devices, it is clear from the literature that the conditions of construction have a tremendous effect on their physical and electrical properties. Thus, a review of the key considerations required to create practical diamond electrodes is warranted.

Discussion will revolve around the use of these electrodes for electroanalysis and electrocatalysis. These are the two most popular applications for boron-doped diamond electrodes (BDE). Non-electronic or electrochemical applications will not be discussed here; however, the methods discussed are applicable to the creation of nano-composite materials in which diamond enhances their physical properties (e.g. improved durability, coating technologies).

Of the many means to modify BDE, only those concerning the construction of NMDE and DNDE will be discussed. These two types of modification have found wide application in the fields of electroanalysis and electrocatalysis. The methods used to construct them have a variety of chemical and physical consequences, which need to be discussed in detail. Finally, we will briefly outline the present state-of-the-art research concerning NMDE and DNDE.

6.2 Metal and Metal Oxide Nanoparticle Coated Diamond Electrodes

6.2.1 Choice of Material

Metals, metal alloys and metal oxides have all been used in electroanalytical and electrocatalytical applications [14], as summarized by Table 6.1 and seen in Fig. 6.1, in the case of Ni(OH)₂ and Pt deposition. Common reasons for choosing a particular material include: chemical aim, chemical environment, compatibility with deposition method, stability, and cost.

The chemical aim is the most important parameter. Metals, metal oxides, and alloys/composites are useful in a variety of chemical systems, as listed in Table 6.1. Notably, Au and Pt are popular materials due to their versatility and catalytic properties. Metal oxides are useful in photocatalytic applications and as alternatives to bimetallic alloys in direct methanol oxidation fuel cells [21]. Bimetallic alloys have advantages compared to their single metal counterparts, whereby metal-metal interactions (e.g. bifunctional mechanism, metal back-bonding) can increase reaction rates and decrease poisoning of reaction sites of a single metal catalyst (see Pt-based alloys in Table 6.1) [22–24]. Chemical aims may require other

Table 6.1 Materials, methods, and applications of nanoparticles on BDE

Material	Method	References	Applications
<i>Metals</i>			
Pt	Spontaneous wet chemical	[57]	H ₂ O ₂ evolution, alcohol oxidation, electroanalysis (arsenite, enzymes), ORR, fuel cell technologies
	Wet chemical assisted	[35]	
	Potential step	[31, 105, 219]	
	CV/potential cycling	[36, 54, 76]	
	Multi-step electrodeposition	[76]	
	Potentiostatic	[31, 36, 43, 105]	
	Microemulsion	[101]	
	Sputtering/ion impact	[40, 63, 64]	
	Thermal salt decomposition	[105]	
	Electrochemical deposition		
	Linear potential sweep	[54]	
	Galvanostatic	[104]	
	Pulsed galvanostatic	[44]	
Sol-Gel	[68, 69]		
Sb	Potentiostatic	[220]	Electroanalysis of heavy metals
Bi	Potentiostatic	[95]	Electroanalysis of heavy metals
Co	Potentiostatic	[79]	H ₂ O oxidation catalyst
	Photoreduction	[221]	
Ni	Potentiostatic	[110]	Alcohol oxidation, biosensing
	Metal implantation	[65, 66]	
Fe	Potentiostatic	[222]	H ₂ O ₂ detection, electroanalysis
Pb	Potentiostatic	[83]	Electroanalysis of heavy metals
Ir	Metal implantation	[64]	Arsenic detection
Ag	Spontaneous deposition	[57]	Perchlorate oxidation, biosensing
Cu	Spontaneous deposition	[57]	Nitrate detection, biosensing, H ₂ O ₂ detection, CO ₂ reduction
	Potentiostatic	[37]	
	Wet-chemical	[181]	
	Potentiostatic coulometry	[38]	
	Metal implantation	[65]	

(continued)

Table 6.1 (continued)

Material	Method	References	Applications
Au	Spontaneous deposition	[57]	Biosensing (proteins, neurotransmitters), ORR catalysis, arsenite detection
	Thermal salt decomposition	[219]	
	Sputtering	[61, 75]	
	Potentiostatic	[55]	
	Self-assembly	[27]	See end of first column
	Linear sweep voltammetry	[77]	
	Electro-aggregation	[223]	
Pd	Spontaneous deposition	[57]	Proton detection, hydrazine detection, ORR catalysis, neurotransmitter detection, C=C and C-C bond hydrogenation catalyst
	Potentiostatic	[50]	
<i>Bimetallic</i>			
Pt/Sn	Microemulsion	[74]	Alcohol oxidation, pollutant degradation
Pt-Ru	Microemulsion	[101, 102]	Alcohol oxidation for fuel cell technologies
	Potential cycling	[54]	
	Sequential and Simultaneous electro-deposition	[34]	
Pt-Au	Sputtering and potentiostatic	[60]	ORR
<i>Metal Oxides</i>			
Pt-RuO _x	Sol-gel	[33, 67]	MOR catalysis, fuel cell technologies
Pt-PrO _x	Multi-step potentiostatic with electrogeneration of oxide	[3]	MOR catalysis, fuel cell technologies
IrO ₂	Thermal salt decomposition	[219]	H ₂ O ₂ detection, pH sensors
	Potential pulsing	[58]	
	Potential cycling	[58]	
	Galvanostatic	[58]	
TiO ₂	Wet chemical adsorption	[111]	Solar cell technologies, H ₂ evolution, detection of maleic acid, Ni ²⁺ , cytochrome c, drinking water purification

(continued)

Table 6.1 (continued)

Material	Method	References	Applications
RuO _x	Sol-gel /electrostatic	[88]	Cl evolution, H ₂ evolution
FeO _x	Sol-gel	[88]	Oxidation of OH ⁻ to O ₂
Ni(OH) ₂	Electrogeneration of OH at Ni particles	[56]	Glucose, MeOH and EtOH oxidation
PbO _x	Electro-deposition with power ultrasound	[107]	Ethylene glycol oxidation
<i>Composites</i>			
Pt-Nafion	Microemulsion with Nafion	[102]	Biosensing
Pt-Dendrimer	Dendrimer encapsulation	[219]	Biosensing
Pt-electropolymers	Electro-deposition/ polymerization	[28, 224]	Biosensing (proteins, neurotransmitters)

considerations. For instance, multi-step reactions may require more than one type of nanoparticle, or the presence of a specific facet, shape or set of interfaces to be present [25, 26]. The chemical effects or compatibility with stabilizers (e.g. Nafion), conductive, and bio-compatible coatings (e.g. SAMs on Au) also need to be considered [27–30].

The chemical environment to which the electrode is exposed will dictate the type of nanoparticles to be deposited. A crucial consideration is the use of toxic metals (e.g. Pb, Ag) on an electrode to be used in biological environments. It may be better to use a non-toxic metal, such as gold. The environment of fuel cells and batteries can be either acidic or alkaline. The dissolution of metal nanoparticles in acids makes their use in the former environment challenging. Metal oxides are an alternative material, due to their increased stability in those harsh environments. For biological applications, metal nanoparticles need to be modified with known organo-metallic chemistry to render it more bio-inert and/or stable at the surface (e.g. SAMs on Au, Ag).

The material must be compatible with the chosen deposition route. For instance, metal nanoparticles are easily deposited using various electrochemical methods. However, the deposition of metal oxides or alloys require more complex methods, such as: multi-step electrochemical routes and sol-gel based methods [14]. The deposition of metal oxides can occur by physical vapour deposition (PVD), with recent advances promising to enable the deposition of core-shell metal oxides onto surfaces (i.e. Mantis Deposition Ltd.).

Ideally, electrodes should be functional more than once. Therefore, the resultant NP-modification must be stable, both physically and chemically. Some nanoparticles, such as platinum, are known to have weak adhesion to diamond, thus motivating the search for their increased stability at BDE [31, 32]. Stability is of utmost

importance in biological environments, where NPs are known to have inflammatory properties in solution. The instability of metals can be resolved by using alternative metal oxides, as exemplified by the replacement of Ti, Ta, Ti-Pd alloys on carbon-based electrodes by RuO₂ for electrocatalysis and chlorine evolution [33].

The cost of materials can be high, particularly those with the best catalytic versatility and performance (e.g. Pt, Au). Although these materials have been shown to be electroactive at extremely low loading rates (i.e. sub-monolayer), any further reduction in cost, without sacrificing performance is attractive [14]. Many strategies are used, including the use of cheaper materials (e.g. Ni, Pb, Sn, Fe, Cu, Co) and the metal oxides [14], as outlined in Table 6.1. It is clear from this table that these alternatives can be used for the same reactions as those of Pt and Au. The use of an alternative material may offer superior performance, or reduce costs by increasing nanoparticle stability and longevity.

6.2.2 *Methods of Deposition*

Ideally, nanoparticles should be deposited in a chemically active form, having small size, uniform distribution, and low mass loading (<10 % of surface coverage); these characteristics are associated with the best performing electrochemical and catalytic diamond-based electrodes [14, 34]. The deposition method chosen is paramount to achieving these results. The deposition methods in Table 6.1 can be generally categorized by whether they utilise electrochemistry or not. These two general approaches are discussed in this section.

6.2.2.1 **Electrochemical Methods**

Electrodeposition, in its various forms, is the most popular route towards metal nanoparticle deposition. These methods share a common feature, with metal cations from the appropriate salt (e.g. H₂PtCl₆) being reduced at the diamond electrode by some applied potential (e.g. Fig. 6.1b) [14]. The deposition is further controlled by the choice of electrochemical method, the deposition time, deposition potential, metal ion concentration, scan rate, and number of deposition phases/stages [14]. The advantages and disadvantages of popular electro-deposition methods are described here.

The potentiostatic method is most popular technique. This is certainly clear from Table 6.1 and noted elsewhere [14]. Simply, it involves the exposure of the electrode to a metal salt solution, followed by deposition at a fixed potential [14]. The deposition conditions, such as applied potential, duration, and metal salt concentration are easily tuned. For instance, it is accepted that deposition time is proportional to mass loading for most nanoparticles [35–39]. An example of this phenomenon is demonstrated by comparing Fig. 6.1a, d in the case of Pt deposition on BDE. The method has disadvantages. As noted in several reports, potentiostatic deposition leads to poor

particle adhesion, large particle size (cf. Fig. 6.1a, d), low mass loading, and inhomogeneous distribution; all these characteristics could result in an impractical diamond electrode, despite decent electrocatalytic performance [32, 40–42].

Changing the electrochemical method is often a useful strategy. Potential step deposition methods, such as cyclic voltammetry (CV), linear sweep voltammetry (LSV), potentiostatic step deposition (PSD), chronoamperometry, and galvanostatic methods have all been used to control Pt deposition on diamond (see Table 6.1). The first three alternatives lead to more uniform size and distribution of Cu and Pt nanoparticles [35–39]. CV and LSV are slow techniques, but Welch et al. [38] have noted that slowly increasing or decreasing the potential during deposition offers better control over nanoparticle nucleation, growth, and mass loading. Chronoamperometry has the advantage of promoting high mass loading of Au particles via enhanced mass transfer effects initiated by its use [42, 43]. Galvanostatic and pulsed galvanostatic methods favour the growth of individual Pt particles, as these methods minimize the overlap of reactant depletion zones [44]; lower pulse times and higher applied currents lead to lower particle size and denser distribution [32, 44, 45].

Multi-step and/or multi-technique deposition is a successful means to minimizing the disadvantages of any single method. The Foord group has shown that the combination of potentiostatic and potentiostatic step deposition enables particles to grow by both instantaneous and progressive nucleation stages [3]. Also, potentiostatic deposition followed by LSV increases and homogenizes particle size [37]. Combining electrodeposition with electropolymerization of a polymeric stabilizer (e.g. Nafion) or conductive polymer (e.g. polyaniline) is an effective route towards stabilizing nanoparticles on the diamond surface [46–48].

Deposition Conditions

The conditions at which deposition occur are extremely important. The most important of which is that the potential applied to facilitate deposition must be sufficient to drive the reduction of metal cations at the electrode [14]. The most systematic studies have been conducted by the Compton group, notably their work on Cu [38, 49], Pt, Pd [50, 51], Ag [49], Au [49], Ir [52] and other metals, as reviewed here [14]. Vinokur et al. [53] demonstrated that the nucleation of Ag and Hg on BDE depends on overpotential. The appropriate applied potential(s) can provide a higher driving force for the deposition reaction, with the consequences of higher nanoparticle nucleation rates, higher nanoparticle densities, and smaller sizes [14, 41].

Caution and thought must be employed when choosing the applied potential(s). Depositing at potentials near that of H₂ or O₂ evolution is problematic, as gas bubbles can dislodge freshly deposited nanoparticles [41]. Also, the potential can have desirable or undesirable *chemical* effects, such as H₂ cleansing of Pt nanoparticles [41], the co-deposition of bimetallic alloys [54], the pre-concentration of other ions at the interface (e.g. OH⁻, H⁺) [3], or the stripping of nanoparticles from the electrode [38]. In addition, the choice of potential has been found to affect the

shape of Au [55], Cu [37], and Pt [34] nanoparticles. Examples of these effects can be seen by comparing Fig. 6.3a, c, as well as Fig. 6.3e, f pairwise. In the first pair, it is clear that applied potential can affect shape, while in the second pair shows that applied potential can affect particle size. For the deposition of metal oxides via an electrochemical route, the choice of deposition potential is essential for the deposition of the nanoparticle *and* the electro-precipitation of the oxide, due to local pH changes at the nanoparticle surface during deposition [3, 56]. This can result in the deposition of nanoparticles with controllable size and morphology compared to sol-gel routes. An example of this electro-deposition is shown in Fig. 6.1a, for the case of Ni(OH)₂.

Other controllable conditions include the length of deposition, the scan rate, the nature of the deposition solution. The length of deposition is generally proportional to mass loading [3, 32] and is known to influence the morphology of deposition, with longer times exploited to great larger particle sizes [32]. In the case of CV, multiple scans can homogenize the size of nanoparticles, but not the particle

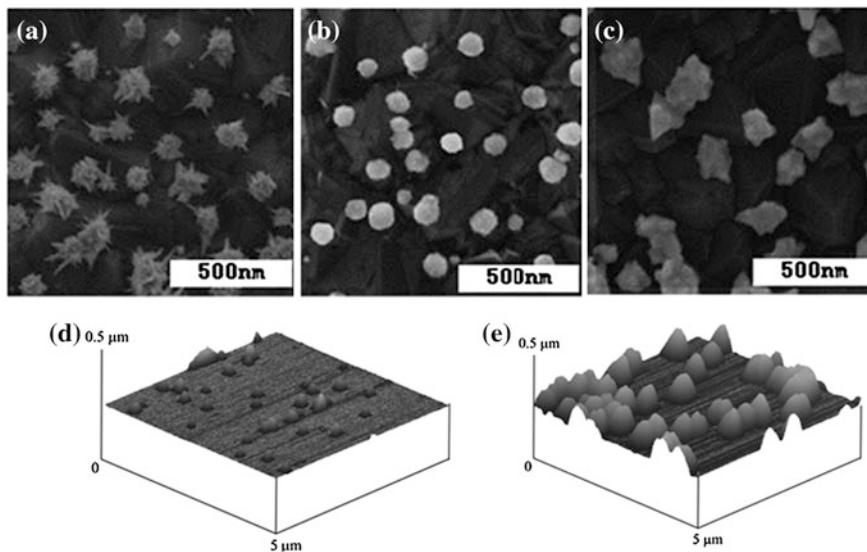


Fig. 6.3 Images of nanoparticles on diamond with electrodeposition influenced by applied potential or concentration of metal salt in solution. (*Top row*) SEM images of gold nanoparticles electrodeposited on boron-doped diamond surfaces: **a** Flower-like Au nanoparticles deposited at +0.5 V versus Ag/AgCl in 0.2 M H₂SO₄ solution containing 2 mM HAuCl₄; **b** Spherical nano-gold deposited at +0.5 V versus Ag/AgCl in 0.2 M H₂SO₄ solution containing 0.2 mM HAuCl₄; **c** Convex polyhedron nano-gold prepared in same conditions as A, except at an applied potential of -0.1 V versus Ag/AgCl. (*Bottom Row*) In situ tapping mode AFM images of cobalt grown on a BDD surface from 10 mM Co(II) at potentials of **e** -1.05 V and **f** -1.15 V. Reprinted from Li et al. [55] with permission from Elsevier (Copyright © 2006). Reprinted from Simm et al. [79] with permission from Wiley-VCH (Copyright © 2006 WILEY-VCH Verlag GmbH & Co. KGaA, Weinheim)

distribution [38]. Adjustment of the scan rate has been shown to promote facet selective deposition of Pt on polycrystalline diamond [39]. At higher sweep rates, particles preferred to deposit on the (111) facet, as dramatically shown in Fig. 6.4. The sweep rate also affected shape and distribution, with the (111) facet having more numerous and smaller particles than the (110) facet. Oxygenated surface moieties are thought to concentrate on (111) facets. As mentioned in other sections, the presence of oxygen functionality increases nanoparticle stability, nucleation, and diamond is more electroactive in such regions [39].

The nature of the solution in which electrodeposition occurs is an important consideration. The concentration of metal ions in solutions seems to affect the nucleation pathway of Ag and Hg deposition [53]. In addition, concentration affects nanoparticle shape. This is shown in Fig. 6.3, where a 10-fold dilution of HAuCl_4 leads to spherical deposition, compared to “flower-like” shape at higher concentrations (see Fig. 6.3a, b) [55]. Adjusting concentration can have unusual effects. For instance, the density of electrodeposited Ag nanoparticles is inversely proportional to size, except at very dilute concentrations of the metal salt [57]. Other adjustments to the type of solution and pH can be made. Additionally, the pH of the solution [27, 58] or local pH at the interface [3, 59] can affect electrodeposition. The latter has been discussed in the previous section for the case of metal oxide deposition.

6.2.2.2 Non-electrochemical Methods

Non-electrochemical methods are used less frequently. They are often complex and require advanced equipment, unavailable in most laboratories. Two of the more common techniques are briefly discussed here.

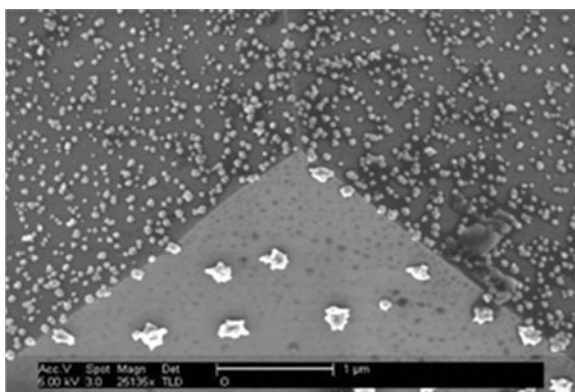


Fig. 6.4 Scanning electron microscopy image of Pt nanoparticles on boron-doped diamond deposited with potential cycling from -0.8 V to $+1.6$ versus Ag/AgCl in 0.5 M H_2SO_4 at a sweep rate of 500 mV/s. The (111) facet edge is clearly visible. Reprinted with permission from Gonzalez-Gonzalez et al. [21], Copyright (2009) American Chemical Society

Physical vapour deposition techniques, such as ion impact and sputtering depositions are effective in vacuo methods for depositing nanoparticles on diamond. Both techniques vaporise metal from a source, but the former accelerates the ions by 800 keV towards the sample, rather than merely coating the surface by physical deposition [14]. Often, these techniques are used to modify CVD diamond films during their creation. For instance, DC magnetron sputtering was used by the Swain group to create Pt-sandwich electrodes, in which a Pt layer was sputtered between two CVD grown layers, halfway through the CVD process [40]. Bimetallic deposition is possible if two or more metal sources are in the vacuum chamber. Uniform nanoparticle distribution is often the result of using a PVD method, as nanoparticle deposition is relatively unaffected by the inhomogeneous distribution of boron at BDE or by grain boundaries [42]. Heat treatment post-PVD deposition may be necessary, as in the case of Au nanoparticles [60–62]. When conducting ion implantation, the modified BDD must be heated by high temperature in the presence of ambient H₂ not necessarily to modify the structure of deposited nanoparticles, but to recover metastable diamond structures produced by the ion bombardment itself [63–66]. By far the greatest advantage of PVD methods is that the ultra-high vacuum conditions reduce unwanted physio-chemical effects (i.e. oxidation, water) on nanoparticles due to solution or ambient conditions. Widespread use of PVD techniques is not possible, due to the cost and complexity of the UHV systems required.

The sol gel method is a popular means to deposit metal oxide nanoparticles on a diamond surface [14, 67–69]. Generally, a metal precursor is stabilized as a colloid in ethanol, or 2 propanol, and then coated onto the electrode by dip-coating, spin-coating, or as a paste. Afterwards, a thermal heat treatment is sufficient to ensure nanoparticle formation having the proper structure. For example, anatase TiO₂ has been deposited onto diamond via this route at thermal heat treatment at 400 °C [70]. While the sol-gel method typically leads to random and uniform distribution of nanoparticles on diamond, it suffers from the disadvantages of large particle sizes and particle aggregation. This is exemplified by the image of Fig. 6.2a, in the case of nanoparticle deposition on diamond nanoparticles. A recently developed alternative to the sol-gel method is the aforementioned electro-precipitation of the oxide, either during a single step [56] or as a coating for pre-deposited nanoparticles [3]. Results suggest that this method offers better control of nanoparticle deposition via electrochemical parameters, the effects of which are discussed in some detail later. Some of the state-of-the-art wet-chemical deposition routes are discussed in Sect. 6.5.

6.2.2.3 Substrate

Thus far, conductive diamond has been referred to simply as BDE. In actual fact, BDE are categorized by the method of their creation and by their crystallinity. More detail than will be described here concerning the manufacturing of BDE can be found in several reviews [1, 4, 9, 71, 72]. The chemical vapour deposition (CVD)

method is most commonly used, and this has several consequences for the deposition of metal and metal oxide nanoparticles on diamond substrates.

CVD diamond is made by ionizing hydrogen and methane with a thermal or microwave source. The ions re-combine on a substrate—often silicon—to form a sp^3 carbon network. Boron doping can be introduced to the diamond film by having a source of boron in vapour form during the CVD process. This manufacture process can be adjusted to make a wide variety of diamond substrates, with different distributions of B doping and crystallinity. The substrate does not affect the nanoparticle growth or distribution tremendously when non-electrochemical methods are used to deposit nanoparticles. Therefore, subsequent discussion concerns itself with the affect substrate has on the electro-deposition of nanoparticles.

Metal nanoparticle nucleation occurs at the most electroactive sites on a diamond surface, such as boron centres, grain boundaries, and defects [14]. Thus, the distribution of B and the dimensions of surface crystals are important factors to be considered. The distribution of boron centres is inhomogeneous, thus partially explaining the non-uniformity of nanoparticle growth when using electrodeposition techniques [44, 45, 73]. This inhomogeneity can be seen in Fig. 6.5a–c. The grain boundaries have increased surface concentrations of electroactive sp^2 carbon and oxygen moieties; thus, denser concentrations of nanoparticles tend to found in these regions [64, 74, 75]. Further increases in nanoparticle density can be achieved by depositing onto BDE with smaller grain sizes (i.e. macro > micro > nano), due to their increased surface area [76]. This trend can be seen by comparing Fig. 6.5c, d. It is thought that this trend explains the effectiveness of lower nanoparticle loadings on micro-crystalline diamond electrode, compared to its macro counterpart [76]. Smaller grain sizes also help to reduce aggregation, reduce particle sizes, and make distribution more uniform, as seen in Fig. 6.5d. This distribution and morphology promotes hemispherical diffusion profiles, which are electrochemically favourable [14, 76]. There is some debate whether metal nanoparticles deposit randomly or non-randomly on polycrystalline diamond, with the work of the Macpherson group suggesting is both random and uniform [43].

Pre-treatment of BDE prior to deposition has been shown to lead to improved nanoparticle stability and electrode performance. Oxygen-terminated diamond stabilizes metal nanoparticles better than hydrogenated diamond [33, 43]. One can add oxygen functionality to the surface by a variety of means, including oxygen plasma and anodic electrochemical treatment [77, 78]. However, passivation of the diamond film by thick overlayers of oxygen is to be avoided. Pre-roughening of the BDE surface can increase surface area, thereby improving nanoparticle adhesion and uptake; this is shown to be effective by Hu et al. [32] who used nanodiamond powder suspensions as the roughening medium.

Interestingly, the diamond surface alone may not necessarily have an effect, but rather the material which supports it. Recently, Gao et al. [57] demonstrated that the spontaneous deposition of Ag, Cu, Au, Pd, and Pt on diamond could be achieved in HF, when the diamond surface was in ohmic contact with hydrogen-terminated silicon. It is thought that this type of contact increases the surface electron energy of diamond, thereby promoting the migration of excess electrons from the silicon/HF

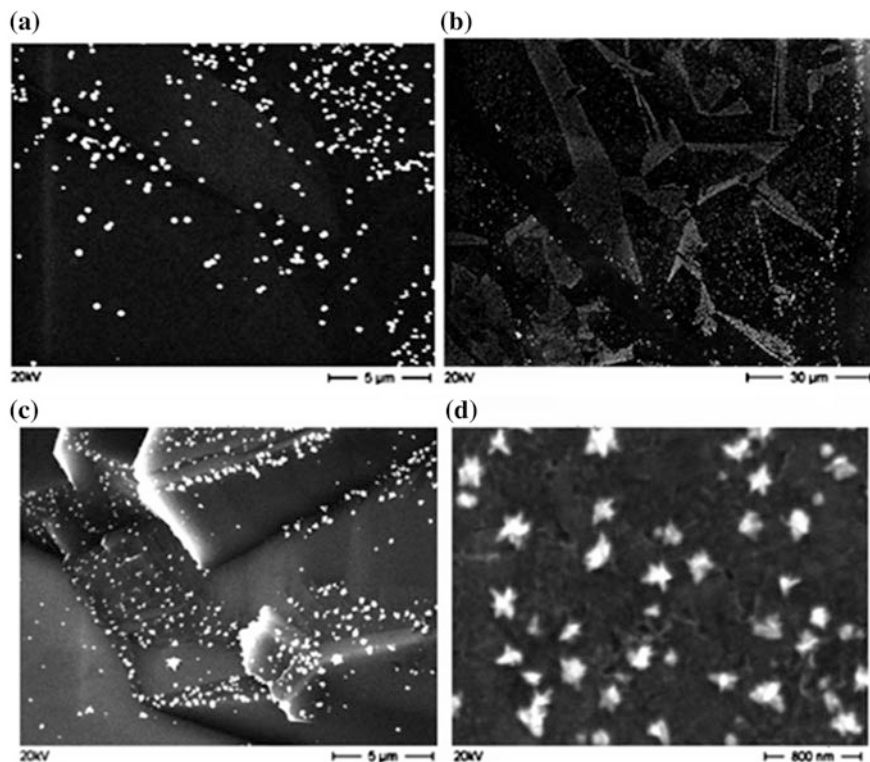


Fig. 6.5 SEM images of platinum deposited on (a, b) polished smooth boron-doped diamond electrode, c as-grown large grain, and d small grain diamond substrates. Reprinted from Hu et al. [31] with permission from Wiley-VCH, Copyright © 2009 WILEY-VCH Verlag GmbH & Co. KGaA, Weinheim

interface to the conductive diamond interface [57]. In this manner, the diamond surface is made more reductive, thereby leading to the spontaneous reduction of metal ions onto the diamond surface. Silicon dioxide was unable to achieve this same effect, thus highlighting the importance of substrate choice to deposition chemistry.

6.2.3 Surface Characteristics

6.2.3.1 Characterization Techniques

Surface characterization of NP-modified diamond films is necessary to both confirm nanoparticle deposition and understand the fundamental surface chemistry of the electrode. The size and morphology of deposited nanoparticles is best studied using

atomic force microscopy (AFM), scanning electron microscopy (SEM), and transmission electron microscopy (TEM). Notably, in situ studies of nanoparticle nucleation and growth are possible using electrochemical AFM (EC-AFM) [14, 79]. The surface chemistry of the deposited nanoparticles can be effectively determined using X-ray photoelectron spectroscopy (XPS), time-of-flight secondary ion mass spectroscopy (ToF-SIMS), and Raman spectroscopy. Crystal structure of both the substrate and the nanoparticles can be determined using X-ray diffraction (XRD). Finally, the electrochemical properties and mass loading of nanoparticles is usually determined by cyclic voltammetry and stripping voltammetry.

6.2.3.2 Nanoparticle Distribution

The distribution of nanoparticles across an electrode can be modified to achieve a given electrochemical or electroanalytic purpose. Higher current densities, higher signal to noise ratios, and higher faradaic to non-faradaic current ratios, occur at surfaces comprising widely-spaced and uniformly distributed nanoparticles [80, 81]. In this case, mass transport of reactants to the nanoparticles occur via fast, three-dimensional, diffusion, as opposed to linear diffusion [76, 80]. These characteristics are known to improve electroanalysis and electrocatalysis at nanoparticle-based electrodes. In cases where macroelectrode performance must be realised at reduced cost, one might distribute nanoparticles more densely (e.g. 50–100 nm particle to particle spacing), to ensure that electron transfer is limited by mass transport (i.e. planar diffusion) of the reactant to the surface, thereby lowering electrode sensitivity [76, 80, 81]. In some cases, the kinetics of electrochemical reactions are paramount; the location and distribution of reactive nanoparticles can control or exploit the interplay between reactant mobility and adsorption [81]. Nanoparticle deposition near active sites, defects, and grain boundaries could be of benefit if such sites are important to the electrochemical system. Finally, the promotion of certain nanoparticle shapes requires preferential growth on certain grain boundaries of diamond [39]. The degree to which particles distributed uniformly can be determined by comparing experimental data to theoretical models [81, 82].

Non-uniform nanoparticle distribution on BDE is promoted by inhomogeneous distributions of boron-centres, grain boundaries, high number of surface defects, and high levels of sp^2 contamination. These surface features are highly electroactive, with nanoparticles nucleating and growing on these sites during electrodeposition [31]. This explains the difficulty of depositing homogeneous distributions of NP by electrodeposition. More uniform distributions are obtained by reducing the number of defects or grain boundaries (cf. Fig. 6.5c, d), and by making the surface less electroactive by increasing the surface density of sp^3 carbon [83]. Some reports do suggest that electrodeposition of nanoparticles can occur grain-independently [43, 83].

Uniform nanoparticle distribution is produced, generally, by non-electrochemical methods of deposition [75]. An alternative is to functionalise the diamond and/or nanoparticle surface prior to deposition, in order to promote uniform nanoparticle

distribution. For example, two dimensional arrays of Au nanoparticles have been created by covalent attachment of citrate-coated Au NPs to an amine terminated diamond surface [84]. More simply, the pre-roughening of the diamond substrates has been shown to promote uniform nanoparticle distribution [32].

6.2.3.3 Nanoparticle Adhesion and Stability

The dissolution of nanoparticles from a diamond support is not desirable, as it leads to instable electrochemical performance and increases the cost of any electrical or catalytical device. Moreover, the introduction of metal ions into biological systems may have toxic effects. Therefore, the question of particle adhesion and stability is crucial.

Better adhesion and stability may be realised by using alternative materials to an initial choice. For instance, in acidic environments, metal nanoparticles can dissolve, therefore metal oxides should be considered for their stability in these environments. Examples of successful replacements include: use of RuO₂ instead of Ti, Ta, Ti-Pd by RuO₂ for chlorine evolution [33]; use of bimetallic or metal oxide nanoparticles instead of Pt nanoparticles [32, 34, 41]. A consultation of Table 6.1 may inspire the search for alternative materials for a given application.

Sandwiching nanoparticles between layers of CVD diamond seems to be the best method for retaining nanoparticles. The classic example is that of Swain et al. [40] who sputtered Pt onto CVD diamond, followed by a period of further diamond growth. The high stability of Pt nanoparticles was due to their being partially buried by diamond overlayers or anchored to the surface by diamond growth around the base of individual nanoparticles. Ion implantation achieves a similar level of stability as high energy metal ions are partially buried into the diamond substrate, as demonstrated for Ni [65], Cu [65], Pt [63], and Ir [64] implantation into BDE. Ion implantation offers 5 month stability, in the best case scenario [65, 85].

Other methods of deposition improve particle adhesion, as noted throughout this chapter. Multi-step potentiostatic methods may be superior to single step potentiostatic methods [3, 14, 76]. Potential pulsing leads to better IrO_x adhesion and is highly recommended for the deposition of metal oxides, compared to galvanostatic or potential cycling methods [58, 86]. Novel wet chemical routes (discussed in Sect. 6.5) also offer the potential for improved particle adhesion and stability [35].

Substrate pre-treatment can also improve particle adhesion and electrode stability. Increasing the surface density of oxygen moieties can improve nanoparticle adhesion [39]. This can be accomplished by pre-treatment in acid, anodic electrochemical treatment, or O₂ plasma [33, 43, 77, 78]. Sol-gel deposited metal oxide nanoparticles and sputter deposited Au nanoparticles have improved adhesion after a heat treatment [60, 62]. Thermal heat treatment can make BDE more hydrophilic, which may be the cause of improved adhesion [87]. Deliberate hydrophilic treatment of diamond lead to improved FeO_x adhesion [58, 88] Ultrasonic pre-treatment

of diamond in suspensions of diamond powders improves the adhesion of Pt nanoparticles [32]. Finally, the careful choice of the type of diamond improves particle adhesion. For instance, Pt nanoparticle modified micro-crystalline diamond outperforms its macro counterpart, providing electroanalytical performance in polluted tap and river water for 150 detection runs [76].

Poorly adhered nanoparticles do not necessarily leave the electrode, but can agglomerate along grain boundaries during an electrochemical experiment. For instance, Pt nanoparticles are stable on the (111) facet of BDD for a few hours during methanol oxidation, but on the (110) facet, particles agglomerate [39]. Agglomeration causes particle size to increase, with the consequence of reduced electrochemical selectivity and sensitivity to analytes, as nanoparticle diffusion layers overlap [14]. It is thought that functional groups on the (111) surface, such as sp^2 carbon and oxygen functionality help to stabilize attached particles [39].

6.2.3.4 Nucleation

The nucleation of materials using electrochemical techniques is still poorly understood and there is much controversy in the field. Hyde and Compton [89] have reviewed some of this debate and recent progress in this area. Due to existing controversy in the field, recent research is discussed in some detail.

Two types of nucleation processes are used throughout the literature on electrodeposition: instantaneous and progressive. The former assumes that nuclei grow slowly on a small number of active sites, simultaneously; the latter assumes that nuclei grow quickly on many active sites, which become activated as the electrodeposition proceeds [89–91]. There exist two methods of determining the nucleation type. The first involves analysing current-time transient curves obtained by chronoamperometry [31, 92]. The second involves the use of in situ EC-AFM [93]. In both cases, the results are most commonly compared to models by Scharifker and Mostany [94]. These models assume a constant nucleation rate and that particle growth is diffusion controlled; depending on the model chosen this can be planar or hemispherical [31, 92, 93].

Diamond is a low energy surface and nucleation is most commonly instantaneous, as exemplified by the electrodeposition of Cu [37], Bi [95], Pt [31, 36, 92] on non-polished, polycrystalline diamond. Instantaneous deposition is driven by high overpotentials and the extent of such nucleation can be controlled by varying the potential [92]. Also, instantaneous nucleation is prevalent on diamond with smaller grain sizes [31, 57]. This can be seen in Fig. 6.5d. Characteristics of instantaneous deposition include: the observation that the number of nucleation sites is controlled by the applied potential [96]; an monotonically broader size distribution during deposition [37], small particle size [37], small particle distribution [41], and the formation of dendritic microstructures on grain boundaries and surface defects [34]. These characteristics helped identify the nucleation type in the

case of Pt and Pt-Ru deposition by sequential potentiostatic methods, compared to deposition of Pt-Ru by simultaneous potentiostatic methods [34].

Progressive nucleation does occur on BDE as well. Platinum deposits onto smooth, polished diamond by a progressive nucleation process, as shown in Fig. 6.5a [31]. These particular nanoparticles are characterised by smooth, spherical morphology with decrease electroactive surface area. By contrast, in the same study, instantaneously nucleated Pt on small and large grain BDE had dendritic structure and higher electroactive surface area (cf. Fig 6.5d). Others characteristics of progressive nucleation include large particle sizes, clustering, and wide size distribution [41, 53, 79]. Some deposition methods may only be capable of progressive nucleation, such as the potential sweep method, in the case of simultaneous or sequential deposition of Pt-Ru onto polycrystalline diamond [34]. Progressive nucleation should be avoided if electrochemical performance is of utmost importance, as instantaneously nucleated particles are more favourable for this application [14].

It is commonly accepted that nucleation occurs most readily at grain boundaries, surface defects, and electroactive sites on the diamond surface, as in the case of Ni and Co [79, 97], Pt [26, 31, 32, 34, 36, 92], Pt-Ru [34], as well as other metal and metal oxides [14]. This phenomenon can be seen in Figs. 6.1, 6.4, and 6.5. The position of nucleation depends on the substrate, particularly the local electroactivity of the surface [31, 32]. On smooth, polished BDE nucleation of Pt may be promoted on the most electroactive facets of diamond [31]. For example, Pt is known to deposit on the (111) facet of polycrystalline diamond (see Fig. 6.4). The size and distribution of grains within the diamond substrate can affect nucleation. Pt nanoparticles are more homogeneously distributed on small grain BDE, compared to large grain BDE (see Fig. 6.5) [31]. The authors attribute this to the higher density of electroactive sites on small grain BDE. Higher boron doping levels make the BDE more electrochemically active [73], and one surmises this would promote instantaneous nucleation; however, to our knowledge this has not been systematically studied yet. Increasing the electroactivity of the BDE substrate is an effective strategy to promote nanoparticle nucleation.

6.2.3.5 Size and Morphology

There is much evidence showing that the best electrochemical performance results from the deposition of small particle sizes (5–10 nm) at low loading rates, with small size distributions [1, 14, 57]. These characteristics ensure a high electroactive surface area, hemispherical diffusion controlled electrochemistry, catalytically active quantum size effects, and the availability of low co-ordinated facets at the surfaces of small particles [14, 75, 98–100]. The above characteristics help ensure the resultant electrode is effective.

Sizes reported in the literature range from 5 nm to 5 μm , with size being controlled in a number of ways. The deposition method can affect the size.

Microemulsion routes [101, 102], wet chemical deposition [57], and the various electrodeposition techniques mentioned in Table 6.1 are capable of depositing nano-sized particles on the order of 2–10 nm. Some PVD methods are capable of depositing similarly sized particles [103]. The use of sol gel methods to deposit metal oxides tends towards large particle sizes, on the order of 0.5–5 μm [67–69]. However, this technique does trend towards low loading rates, on the order of $10^{13} \text{ mol}^{-1} \text{ cm}^2$, [87] thereby minimizing diffusion zone overlap of particles [14].

Many electrodeposition methods have been evaluated for their ability to control particle size, as noted by Hu et al. [31], including: chronoamperometry [43], cyclic voltammetry [38, 54], galvanostatic [104], pulsed galvanostatic [44], potentiostatic step [105], and potentiostatic coulometry [38]. These methods were used to control the size of various metal systems, including: Cu [38, 49], Pd [50], Ag [49], Au [49, 77], Ir [52, 106], and Pb [107]; other systems of interest can be found from Table 1.1 and in other reports [14].

Potentiostatic methods are better able to fine-tune the growth of metal nanoparticles [31, 32, 108]. For example, for the deposition of Cu^{2+} , Ag^{2+} , and Pb^{2+} , potentiostatic coulometry is a superior method to cyclic voltammetry [38]. The latter is known to incompletely strip metal sites, thus promoting uncontrolled growth of metal nanoparticles on pre-existing metal on the surface. Metal is a more energetically favourable deposition site than BDE [38, 109]. In potentiostatic coulometry, only nanoparticles on non-electroactive sites are incompletely stripped, thus ensuring that particle growth is controlled by the electrochemistry of the diamond substrate, alone [38].

Multi-step electrodeposition can be a useful means to achieve better size control, by minimizing the disadvantages of any single method. For example, to adjust size more quickly, the Ford group utilizes a two stage process. In the first stage, nano-sized Pt nuclei are created by the slow increase of negative potential, followed by the application of a fixed potential to enlarge the nuclei to the desired size [3]. The size of metal oxides can be controlled in a third electrodeposition step, in which the oxide is precipitated at the metal nuclei, as done for the case of Pt-PrO_x [3].

Many deposition parameters are reportedly able to change the size of deposited particles, including: overpotential [3, 31, 38, 76, 97], metal ion concentration in the electrolyte [53, 57, 76, 110], deposition time [3, 31, 38, 76, 110], grain size of diamond substrate [43], solution acidity [57] and number of electrodeposition steps [76]. Of these parameters, the most important is overpotential, due to its influence on the energetics of the electrodeposition process, nucleation, and mass transport to electroactive sites on the substrate [14, 34]. Adjustment of the scan rates can homogenize size distribution after initial deposition [37]. Those deposition parameters which lead to instantaneous nucleation are typically those that create the smallest particle sizes, as described earlier. Progressive nucleation leads to the largest particle sizes [110].

There are several other parameters used to control size in the case of non-electrochemical methods. Heat treatment is capable of changing the size of metals,

such as Au, post-deposition [75]. Also, the facet to which the metal nanoparticle adheres may influence size. For example, it has been shown that Pt nanoparticles on (110) facets have larger particle diameter, while those on the (111) facet are smaller in size (see Fig. 6.4) [39]. In this same study it was shown that merely changing the sweep rate during deposition by cyclic voltammetry is sufficient to change the preferred facet of deposition, and thus the particle size [39]. Figure 6.4 shows the result of using the highest scan rate in that study.

6.2.3.6 Shape

Performance can be further enhanced by changing the morphology of deposited nanoparticles. A number of different shapes and particle morphologies have been made on diamond, including: convex polyhedron (see Fig. 6.3c), flower-like or dendritic (see Fig. 6.3a), spheres (see Fig. 6.3b), clusters, and agglomerations. The size of these features varies from the nano-scale to the micro-scale, depending on the system studied. Shape can be controlled in a number of ways, including: deposition type, nucleation type, overpotential, metal ion concentration, and linear sweep rates. The shape can expose favourable facets of the nanoparticle to the solution and increase the exposed surface area, both of which are desirable features for a modified BDE [55].

There are several reports showing that deposition type can control particle shape. Deposition from sol gels and microemulsion tend to form clusters and agglomerates of metal oxides and metals at BDE [57, 67, 111]. Dendritic and smooth particles result from potentiostatic and linear potential sweep methods, respectively [31, 54]. In multi-step methods, one might consider the effect of simultaneous versus sequential deposition. For example, they lead to spherical and dendritic structure, respectively, in the case of Pt-Ru deposition [34].

Other deposition parameters can be optimized to favour certain shapes. Flower and dendritic growth is promoted by instantaneous nucleation, while spheres, clusters and agglomerations are more prevalent during progressive nucleation [18, 34, 55, 75, 95]. The parameters which favour one or the other type of nucleation have been discussed earlier. Dendrite formation requires prismatic growth in the early stages of deposition and is related to overpotential [57, 112]. This may be due to the fact that higher overpotentials cause near maximum mass transport limits [113]. For example, at constant metal ion concentration, a simple change in overpotential is capable of changing Au deposition shape from flower-like to a convex polyhedron (cf. Fig. 6.3a, c) [55]. Also, heat treatment has been used to change the shape of Au nanoclusters and does so by exposing the nanoparticles to the very electroactive Au(111) plane, which promotes dendritic-like growth [75].

During the spontaneous deposition of Ag, Cu, Au, Pd, Hg, and Pt onto Si supported BDE, it was found that metal ion concentration is key to particle shape [57]. The authors note that dendritic, small spheres, and large spheres were related

to high, low, and dilute concentrations, respectively. In the case of dilute concentrations it is more favourable for metals to deposit onto metal rather than the underlying BDE electrode, thereby increasing particle size [57]. High and low concentrations of HAuCl_4 were found to lead to ‘flower-like and spherical nanoparticle shapes on BDE (cf. Fig 6.3a, b) [55].

6.3 Diamond Nanoparticles as an Electrode Material

Detonation nanodiamond (DND) is of emerging interest, with research finding it to have a diverse set of applications, including biomedicine, catalysis, quantum computing, nano-composites, and for the seeding of CVD diamond growth [5]. It has a number of attractive features, including optical transparency, large surface area, and a bio-compatible sp^3 core structure. These characteristics make DND a material of choice for use in bio-medical implants, nano-scale electrochemistry, drug delivery, cell imaging technologies, and as a substrate for cellular growth [5, 20, 114–117]. The myriad of applications of nano-scale diamond has been reviewed by Holt [5] and Schrand [20].

6.3.1 Background on Detonation Nanodiamond

Lewis et al. [118] first found diamond nanoparticles in interstellar dust and meteorites. Since then, efforts have been made to create nano-scale diamond particles, synthetically by the controlled combustion of explosives. Nanoparticles of diamond are synthesized by the controlled combustion of explosives in high oxygen conditions [20, 116, 119]. These particles undergo cleaning processes (i.e. acid treatment, oxidation by Ostwald method [120] to remove metal impurities and to reduce their size to primary particles, they must undergo deaggregation [20].

The resultant material is comprised inner, sp^3 diamond core of 4–5 nm and an outer shell of non-diamond character, with complex surface chemistry [121]. This outer shell of purified DND contains a mixture of sp^2 and sp^3 carbon [122] and oxygen based functional groups (i.e. carboxylic acids, esters, lactones) [20]. If desired, this surface chemistry can be changed by fluorination [123], hydrogenation [124], and the attachment of alkyl, amino, and amino acid groups [123, 125]. The physical and chemical properties of DND depend strongly on the size of the nanoparticles [124], with size control of the DND required for the stabilization of their colloidal suspensions [126] or to ensure specific reactivity [127, 128]. The surface area of primary sized DND is approximately $270\text{--}280\text{ m}^2\text{ g}^{-1}$ [129], thus providing greater surface area for nanoparticle attachment than conventional diamond films.

6.3.2 Electrochemistry of Detonation Nanodiamond

DND is an undoped form of diamond. One normally associates undoped diamond as being an insulator and impractical for use in an electronic device. Unlike the bulk material, DND is electrochemically active in its undoped form. Like many materials, the nano-sized version exhibits different chemical properties than its bulk form. This is due to its high surface area, multi-faceted nature, and its outer shell, which contains reactive sp^2 carbon and oxygenated functionality [126].

Commercial DND particles of primary particle size are redox active, but not in a classical sense. The classical picture considers that H-terminated diamond is redox active, if chemical potentials are below the valence band maximum [130, 131]. Also, it considers that p-type conductivity at the surface exists due to electron transfer between H-termination and dissolved oxygen in aqueous environments [132]. This is not true of DND, as determined by Holt and her colleagues in 2008 and 2009.

Our understanding of DND redox behaviour has been advanced by the Holt Group who have conducted extensive electrochemical studies of commercial DND (5 nm) [19, 133]. They found DND to have ‘molecule-like’ redox behaviour [19]. That is to say that the particles themselves undergo oxidation and reduction via surface states at specific potentials [19]. It is easier to reduce DND particles than to oxidise them [133]; this process is spontaneous and slow in the presence of certain redox species without an applied potential [19, 133]. The electrochemical behaviour may also be due to the presence of sp^2 carbon, delocalised electrons due to oxidation, and unsaturated bonding of surface atoms; all this gives DND surfaces a semiconductor/metallic character [133]. Although doping of DND particles is possible [134, 135], it is not required for the vast majority of its electrochemical applications, due to its intrinsic redox behaviour.

6.3.3 Methods of Deposition/Incorporation into Electrode Form

There are several methods available to make DND particles into a useful electrode. DND particles have been placed on Au electrodes by drop coating from ethanol suspensions [19] and on glassy carbon electrode by smearing a DND-mineral oil paste on its surface [19, 136, 137]. The former method leads to non-uniform coverage and DND agglomeration, while the latter method formed a thin uniform layer on the electrode [19]. Thin coatings are particularly important, in order to avoid electrochemical blocking effects by the DND particles on the glassy carbon electrode [19]. A DND electrode can be manufactured by grinding DND powder into the tip of a Pt wire sealed in a small pipette [136].

More sophisticated electrodes are in existence. For instance, DND has been electrophoretically deposited as thin uniform layers [138]. As well, DND-polyaniline

composites have been made by sequential and simultaneous deposition processes [139–142]. Interestingly, these methods lead to the nanostructuring of PANI in one-dimension, as the PANI oligimers aggregate under the influence of pi-pi stacking [142]. This result hints that DND co-deposited with other materials can lead to novel materials with interesting chemical properties. Non-contact microprinting [143] and layer-by-layer self-assembly by a high pressure/high-temperature methodology [144]. It has been theorised the DND can be electrodeposited onto electrodes [145], but to our knowledge this has not been evaluated in practice.

One example of co-deposition is the modification of diamond with metal or metal oxide nanoparticles, as discussed in this review. DND has also been modified with nanoparticles in a similar way, for similar applications (see also Table 6.1). Supporting catalysts on nanodiamond will benefit from the high surface area and increased reactivity of nanodiamond, compared to its bulk form. Thus, lower loading rates are required to make a practical electroanalytical or catalytic device, based on nanodiamond powders. This promises to reduce device costs.

Ni [146, 147], Sn/Pb alloys [148], TiO₂ [149], Pt [150], metal oxides [67], Pt/Ru [34, 151, 152] have been supported on nanodiamond powder based electrodes. Fruitful research can continue in this area, inspired by the work done on bulk diamond. In addition, further optimisation of particle loading, stability, and electroactivity of nanodiamond supported catalysts is necessary.

6.3.4 Characterization of Diamond Nanoparticle-Based Electrodes

Nanodiamond powder films on surfaces have been characterized by SEM and AFM [152, 153]. Nanoparticle layers form porous sub-micron structures, which enhances its electroactivity compared to bulk films [152]. Holt et al. have characterized DND films by FTIR, XPS, TEM, and Raman spectroscopy [19]. Graphite G and D bands in Raman spectroscopy indicate the presence of surface sp² carbon [19]. XPS shows the oxygenated character of the nanodiamond surface [19]. Nanodiamond has also been characterized by scanning electrochemical microscopy (SECM) [133]. Redox behaviour at diamond nanoparticles has also be evaluated by in situ infrared spectroscopy [154].

6.4 Interactions at the Metal-Diamond Interface

Interactions between diamond, in its various forms, and the nano-materials discussed in this review are key to the understanding of the stability and electronic performance of these composite systems. Diamond has no native oxide, and therefore the electronic behaviour of its surface is highly dependent on any surface modification. Doping of diamond films with impurities which induce p or n-type

doping transforms an otherwise insulating material into a semi-conductor. Redox active species at diamond surfaces (i.e. COOH, C–O–C, lactones, ketones) are known to facilitate electron transfer between the diamond interface, an electrolyte, and metal ions [155]. The above are all well-known phenomenon; however, there is a lack of systematic and fundamental research concerning other, more complex phenomena at the metal-diamond interface [25, 156]. A review of some progress in this area is presented here.

The manufacturing process, polishing, cleaning, and exposure to ambient environments can introduce impurities to the diamond surface. In the case of DND particles, the level of impurities can reach 10–12 % of the total surface area [157]. Examples of these impurities include sp^2 carbon, organic-based functionality (O, N, S, B), metal salts, and defects, among others [157]. Some impurities can lead to favourable interactions. For example, metals with a preference for the +2 oxidation state (e.g. Ni, Ti, Cu, Co, Fe, Al) are thought to be stabilized by interactions with oxygen groups, such as carboxyls and hydroxyls [14, 97, 157–159]. These functional groups, in close proximity to each other on DND particle surfaces have been found to participate in ion exchange with metals in the +2 state, as determined by ^1H and ^{13}C NMR [159, 160]. This is evidence for non-covalent bonding between oxygen-based impurities and metal nanoparticles. Covalent bonding is also possible, as in the case of Al bonding to DND nanocrystals via carboxyl terminations, thereby leading to aggregation of DND in solution [157]. Carbide bonding, such as that between diamond surfaces and Au/Ti, Al, and Ti are known to improve contact resistance and mechanical properties, as determined by the circular transmission line method (c-TLM) [161]. However, not all impurity-metal bonding has a purpose or is favourable. For instance, metal bonding to sp^2 carbon is known to interfere with the electrical properties of the diamond electrode and it reduces the strength of metal-diamond adhesion [162].

Electrostatic effects are thought to play a role in governing metal deposition and stability on diamond-based electrodes. O-terminated and H-terminated DND particles have negative and positive zeta potential over a large pH range (up to pH 12) [128, 157], and this may govern the dynamics of electropositive or negative metal ions to their surfaces. Facet dependent deposition of metal and alloy nanoparticles onto diamond thin films has been observed for a variety of systems (Au, Pt, and their alloys) [39, 156]. The reason for this behaviour seems to lie in the differing electrostatic properties of the various facets [39, 156]. This is supported by the finding that for DND particles sp^3 carbon (i.e. 100 orientation) is electropositive, while sp^2 carbon (i.e. 111 orientation) is electronegative [135].

Electronic interactions between diamond and metal nanoparticles have been observed. For example, the electrical potential of DND nanoparticles are affected by the substrate, size, height, and surface termination [163]. Stehlik et al. [163] observe that the work function diamond interfaces are altered when an electric dipoles (i.e. added metal nanoparticles) is added, thus changing the energy electrons require to reach the vacuum level.

Metallization is a useful change in the electronic properties of conductive diamond, as it improves charge transfer between diamond and any surface modifier [155].

Calculations based on Density Functional Theory (DFT) and experimentation have shown that the band gap is removed if modified by metals, O-terminated diamond, and/or sp^2 functionality [157, 164]. Also, the type of electrical contact improves charge transfer. Ohmic contacts between metals and diamond have been associated with better particle adhesion, higher bond strengths, and shorter bond lengths [164, 165]. This is possible for Ti, V, and Ta deposition, but not for Au or Pd deposition [115, 161]. Likely, charge density on carbon is facilitating backbonding to some metals [164, 165], with metals having more unpaired d orbitals (i.e. V, Ta, Ti) and filled d orbitals (Au, Pd) having stronger and weaker electronic interactions with diamond, respectively [164, 165].

There are other lesser known, or studied, electronic interactions between metals and diamond. These include: negative electron affinity [165–167], conductive surface protrusions [168], non-diamond sp^2 [167], conductive diamond to metal backbonding [165], intrinsic structural effects [167, 169], charge trapping/transfer [155, 163], and interpretations based on energy level confinement within quantum dots for particles <7 nm in size [163]. Plana et al. [155] note that many of these same reasons are applicable to the metal-diamond interface, in addition to electrochemical (e.g. electrolyte, double layer) and nanostructural effects. Other subtle effects are possible, such as quantum effects and metal-vacuum properties, as noted by Tyler et al. [166] in their study on electron emission from diamond nanoparticles on metal tips. The size of the metal or diamond nanoparticle is an important parameter to consider when studying any of the above effects [163]. Quantum-based and crystallinity-based arguments may have greater explanatory weight for metal-diamond interactions involving sub-5 nm nanoparticle sizes [81, 127, 163]. More research in this sub-field is necessary to truly isolate the electronic effects at the metal-diamond interface.

Some metal-diamond interactions have physical consequences. The catalytic etching of nano-sized features in diamond surfaces occurs in H_2 environments at elevated temperatures (>700 °C) [170]. Annealing diamond thin films after it has been modified with metal nanoparticles by ion bombardment can lead to the diffusion of metal nanoparticles from the bulk to the surface [14]. Metal adatoms could have preferred deposition sites, as suggested by DFT calculations of Ti on diamond (100), whereby Ti prefers pedestal sites on top of carbon dimer rows [162]. Annealing of surfaces leads to metal-diamond aggregates involving DND particles, which may be the result of covalent bonding between DND particles with metal ions acting as linkers [157].

6.5 Modern State-of-the-Art and Outlook

Research on the modification of diamond electrodes with metal and metal oxides, continues apace. Research in the past three years has been motivated by interest in fuel cell technologies, photocatalysis and water-splitting, and biological applications.

To our knowledge, two understudied areas of research concern the nanoparticle-diamond interface: the effect of doping levels and the use of epitaxial diamond. Most researchers use commercial BDE and do not investigate how doping levels, doping elements, or type of doping affect nanoparticle deposition. Secondly, studies of nanoparticle deposition on epitaxial diamond could prove fruitful. It is known that the diamond (111) facet is preferred for nanoparticle deposition and such deposition leads to enhanced electrochemistry. The fundamental chemistry of that interface is important, but little understood. One group has attempted to study the role of doping on epitaxial grown diamond [171]. However, more systematic studies, such as that done by Holt et al. [73] on the effect of doping levels for unmodified (i.e. H-terminated diamond) need to be made for the case of diamond electrodes modified with nanoparticles.

Renewable energy technologies are of high interest in the 21st century and new materials are sought to address challenges in environmental and energy technologies. The use of organo-metallic ligands to either aid in the deposition process or to support nanoparticles at the surface, has led to novel electrodes. Porphyrin rings stabilize the deposition of various metals, including Co and Ru, known to be effective in dye-sensitized solar cells and CO₂ reduction fuel cells [172–174]. The deposition of TiO₂ nanoparticles on BDE and DND is considered a promising approach for photocatalysis, water-splitting, and water treatment based on solar energy [149, 175–177]. Bimetallic nanoparticles deposition remains important for alcohol oxidation in fuel cells (Pt-Ru [34, 151, 152]) and nitrate reduction (Cu-Sn [178], Cu-Pd [178]). Nanoparticles which equal the effectiveness of Pt nanoparticles, with better stability, have yet to be discovered. Therefore, much recent effort has been expended in realizing the increased stability and reduction of fouling on Pt nanoparticles for electrocatalytic applications [3, 31, 32, 34, 35, 39, 41, 92, 151, 152, 171, 179, 180].

Recently, there has been a resurgence of interest in wet-chemical routes towards depositing metal nanoparticles on carbon-based materials. In particular, the reduction of metal precursors to metal nanoparticles at a reducing agent attached to an underlying carbon-based surface has emerged as a promising deposition route [151, 181–183]. This method was first attempted at diamond thin films by the Nebel group who seeded the substrate with Pt by reducing H₂PtCl₆ at diamond modified by NaBH₄ [35]. Surface coverage and size can be controlled by the number of repetitions of the above process. Further control of size was possible via electrochemical growth processes [35]. The advantage of this approach is the realisation of homogenous distribution of nanoparticles on diamond, which is difficult using non-physical deposition techniques. This approach is likely to have wider application, as exemplified by the modification of nanodiamond with nano-sized (2–5 nm), and homogeneously distributed, Pt and Pt-Ru particles [182]. Wet-chemical assisted deposition of nanoparticles could be easily developed further, considering the existing literature on wet-chemical routes for modifying diamond [184–186].

In the past ten years, many have recognized the potential for diamond-based devices to be integrated into biological systems. This might be imagined as a direct-connection (i.e. neurological stimulation [187, 188]), stimulation of bio-molecules

(e.g. redox of proteins [189, 190]) or for biosensing [56, 179, 191–194]. Zirconia has been used to modify diamond for DNA detection by the Foord group [195]. Several reports exist showing the effectiveness of nickel and nickel hydroxide nanoparticles for glucose oxidase sensing [56, 196]. An array of self-assembled Au nanoparticles has been able to engage in direct electrochemistry with a microbe, thus suggesting more exotic use of diamond within microbial fuel cells [197]. Many reviews exist on this topic, and a selection is provided here [4, 12, 15, 20, 72, 198].

The principle of introducing nano-scale materials to diamond is also applied when proteins [189, 190, 199, 200], enzymes [191] or aptamers [201–203] are attached to the surface. This aids the detection of redox events and molecules at the diamond surface. Particularly exciting is the creation of a diamond FET-based device for HIV. For example, the attachment of cytochrome c on BDE enables cyanide and arsenic to be detected [204]. The applicability of bio-modified diamond-based electrodes to clinical HIV detection was recently shown by Rahim Ruslinda et al. [201]. Diamond is poised to be a material of choice for the integration of solid-state and biological phenomena.

Nanoparticles of metals, metal oxides, or diamond can be easily damaged by physical means. Moreover, their preparation time can be lengthy. Various attempts are being made to address one or both of these issues by the following approaches: nano-structuring diamond [205–208], synthesizing new diamond-based nanoparticles (e.g. nanowires [209–211], nanograss [212]), grafting diamond nanoparticles [213, 214], micro-contact printing of diamond nanoparticles to surfaces [143], and the self-assembly of nanoparticles [197, 215–217]. The stabilization of nanoparticles with electropolymers continues to be a fruitful area of research, particularly for bio-applications [139–142, 193].

This chapter reviewed the methods used to construct boron-doped diamond electrodes. The methods and principles discussed here are applicable to the realisation of practical diamond-based electrodes which exploit the nano-scale, either via the deposition of nanoparticles or by having nanoparticle form. By understanding the chemical and physical consequences of any given methodology, one should be able better optimise diamond electrodes to address the biological, environmental, and industrial challenges of the 21st century.

References

1. R.G. Compton, J.S. Foord, F. Marken, Electroanalysis at diamond-like and doped-diamond electrodes. *Electroanalysis* **15**(17), 1349–1363 (2003). doi:[10.1002/elan.200302830](https://doi.org/10.1002/elan.200302830)
2. J. Rubio-Retama, J. Hernando, B. Lopez-Ruiz, A. Hartl, D. Steinmuller, M. Stutzmann, E. Lopez-Cabarcos, J.A. Garrido, Synthetic nanocrystalline diamond as a third-generation biosensor support. *Langmuir* **22**(13), 5837–5842 (2006). doi:[10.1021/la060167r](https://doi.org/10.1021/la060167r)
3. L. Chen, J. Hu, J.S. Foord, Electrodeposition of a Pt-PrO₂-x electrocatalyst on diamond electrodes for the oxidation of methanol. *Phys. Status Solidi (a)* **209**(9), 1792–1796 (2012). doi:[10.1002/pssa.201200049](https://doi.org/10.1002/pssa.201200049)

4. A. Kraft, Doped diamond electrodes. New trends and developments. *Jahrb. Oberflächentech.* **63**, 85–95 (2007)
5. K.B. Holt, Diamond at the nanoscale: applications of diamond nanoparticles from cellular biomarkers to quantum computing. *Philos. Trans. Roy. Soc. A* **365**(1861), 2845–2861 (2007). doi:[10.1098/rsta.2007.0005](https://doi.org/10.1098/rsta.2007.0005)
6. J. Wolters, G. Kewes, A.W. Schell, N. Nuesse, M. Schoengen, B. Loechel, T. Hanke, R. Bratschitsch, A. Leitenstorfer, T. Aichele, O. Benson, Coupling of single nitrogen-vacancy defect centers in diamond nanocrystals to optical antennas and photonic crystal cavities. *Phys. Status Solidi (b)* **249**(5), 918–924 (2012). doi:[10.1002/pssb.201100156](https://doi.org/10.1002/pssb.201100156)
7. M. Amanda, Schrand, A. Suzanne, Ciftan Hens, O.A. Shenderovab, Nanodiamond particles: properties and perspectives for bioapplications. *CRC Cr. Rev. Sol. State* **34**(1–2), 18–74 (2009). doi:[10.1080/10408430902831987](https://doi.org/10.1080/10408430902831987)
8. V.Y. Dolmatov, Detonation synthesis ultradispersed diamonds: properties and applications. *Russ. Chem. Rev.* **70**, 607–626 (2001). doi:[10.1070/RC2001v070n07ABEH000665](https://doi.org/10.1070/RC2001v070n07ABEH000665)
9. A. Kraft, Conductive diamond layers. Production, properties, and possible uses of new electrode materials. *Jahrb. Oberflächentech.* **61**, 109–120 (2005)
10. K.I.B. Eguiluz, J.M. Peralta-Hernandez, A. Hernandez-Ramirez, J.L. Guzman-Mar, L. Hinojosa-Reyes, C.A. Martinez-Huitle, G.R. Salazar-Banda, The use of diamond for energy conversion system applications: a review. *Int. J. Electrochem.* **675124**, 675120 pp. (2012). doi:[10.1155/2012/675124](https://doi.org/10.1155/2012/675124)
11. J-b Zang, L. Dong, Y-h Wang, Review on electrochemical property and surface modifications of nanodiamond powders. *Yanshan Daxue Xuebao* **36**(2), 95–102 (2012)
12. H. Yuen Yung, C. Chia-Liang, C. Huan-Cheng, Nanodiamonds for optical bioimaging. *J. Phys. D Appl. Phys.* **43**(37), 374021 (2010). doi:[10.1088/0022-3727/43/37/374021](https://doi.org/10.1088/0022-3727/43/37/374021)
13. N. Fujimori, T. Imai, A. Doi, Characterization of conducting diamond films. *Vacuum* **36** (1–3), 99–102 (1986). doi:[http://dx.doi.org/10.1016/0042-207X\(86\)90279-4](http://dx.doi.org/10.1016/0042-207X(86)90279-4)
14. K.E. Toghil, R.G. Compton, Metal nanoparticle modified boron doped diamond electrodes for use in electroanalysis. *Electroanalysis* **22**(17–18), 1947–1956 (2010). doi:[10.1002/elan.201000072](https://doi.org/10.1002/elan.201000072)
15. Y. Zhou, J. Zhi, The application of boron-doped diamond electrodes in amperometric biosensors. *Talanta* **79**(5), 1189–1196 (2009). doi:[10.1016/j.talanta.2009.05.026](https://doi.org/10.1016/j.talanta.2009.05.026)
16. I.A. Novolelova, E.N. Fedorishena, E.V. Panov, Electrodes from diamond and diamond-like materials for electrochemical use. *Sverkhverd. Mater.* **1**, 32–50 (2007)
17. S. Szunerits, R. Boukherroub, Investigation of the electrocatalytic activity of boron-doped diamond electrodes modified with palladium or gold nanoparticles for oxygen reduction reaction in basic medium. *C.R. Chim.* **11**(9), 1004–1009 (2008). doi:[10.1016/j.crci.2008.01.015](https://doi.org/10.1016/j.crci.2008.01.015)
18. S.R. Belding, F.W. Campbell, E.J.F. Dickinson, R.G. Compton, Nanoparticle-modified electrodes. *Phys. Chem. Chem. Phys.* **12**(37), 11208–11221 (2010). doi:[10.1039/c0cp00233j](https://doi.org/10.1039/c0cp00233j)
19. K.B. Holt, C. Ziegler, D.J. Caruana, J. Zang, E.J. Millan-Barrios, J. Hu, J.S. Foord, Redox properties of undoped 5 nm diamond nanoparticles. *Phys. Chem. Chem. Phys.* **10**(2), 303–310 (2008). doi:[10.1039/b711049a](https://doi.org/10.1039/b711049a)
20. A.M. Schrand, S.A.C. Hens, O.A. Shenderova, Nanodiamond Particles: Properties and Perspectives for Bioapplications. *CRC Cr. Rev. Sol. State* **34**(1–2), 18–74 (2009). doi:[10.1080/10408430902831987](https://doi.org/10.1080/10408430902831987)
21. I. Duo, C. Comminellis, S. Ferro, B.A. De, Conductive metal-oxide nanoparticles on synthetic boron-doped diamond surfaces, in *Catalysis and Electrocatalysis at Nanoparticle Surfaces* (Marcel Dekker, New York, 2003), pp. 877–906
22. B. El Roustom, G. Siné, G. Fóti, C. Comminellis, A novel method for the preparation of bi-metallic (Pt–Au) nanoparticles on boron doped diamond (BDD) substrate: application to the oxygen reduction reaction. *J. Appl. Electrochem.* **37**(11), 1227–1236 (2007). doi:[10.1007/s10800-007-9359-4](https://doi.org/10.1007/s10800-007-9359-4)
23. M. Watanabe, S. Motoo, Electrocatalysis by ad-atoms: Part II. Enhancement of the oxidation of methanol on platinum by ruthenium ad-atoms. *J. Electroanal. Chem. Interf. Electrochem.* **60**(3), 267–273 (1975). doi:[http://dx.doi.org/10.1016/S0022-0728\(75\)80261-0](http://dx.doi.org/10.1016/S0022-0728(75)80261-0)

24. K.-W. Park, J.-H. Choi, B.-K. Kwon, S.-A. Lee, Y.-E. Sung, H.-Y. Ha, S.-A. Hong, H. Kim, A. Wieckowski, Chemical and electronic effects of Ni in Pt/Ni and Pt/Ru/Ni alloy nanoparticles in methanol electrooxidation. *J. Phys. Chem. B* **106**(8), 1869–1877 (2002). doi:[10.1021/jp013168v](https://doi.org/10.1021/jp013168v)
25. T. Kondo, K. Hirata, T. Kawai, M. Yuasa, Crystal-face-selective supporting of metal nanoparticles on polycrystalline diamond thin film. *Pacific Chem. Conf. (ANYL-616. American Chemical Society)* (2010)
26. I. Gonzalez-Gonzalez, E.R. Fachini, M.A. Scibioh, D.A. Tryk, M. Tague, H.D. Abruna, C.R. Cabrera, Facet-selective platinum electrodeposition at free-standing polycrystalline boron-doped diamond films. *Langmuir* **25**(17), 10329–10336 (2009). doi:[10.1021/la8035055](https://doi.org/10.1021/la8035055)
27. R.-H. Tian, T.N. Rao, Y. Einaga, J.-F. Zhi, Construction of two-dimensional arrays gold nanoparticles monolayer onto boron-doped diamond electrode surfaces. *Chem. Mater.* **18**(4), 939–945 (2006). doi:[10.1021/cm0519481](https://doi.org/10.1021/cm0519481)
28. M.-J. Song, J.H. Kim, S.K. Lee, J.-H. Lee, D.S. Lim, S.W. Hwang, D. Whang, Pt-polyaniline nanocomposite on boron-doped diamond electrode for amperometric biosensor with low detection limit. *Microchim. Acta* **171**(3–4), 249–255 (2010). doi:[10.1007/s00604-010-0432-z](https://doi.org/10.1007/s00604-010-0432-z)
29. M. Wei, Z. Xie, L. Sun, Z.-Z. Gu, Electrochemical properties of a boron-doped diamond electrode modified with gold/polyelectrolyte hollow spheres. *Electroanalysis* **21**(2), 138–143 (2009). doi:[10.1002/elan.200804411](https://doi.org/10.1002/elan.200804411)
30. M. Wei, L.-G. Sun, Z.-Y. Xie, J.-F. Zhi, A. Fujishima, Y. Einaga, D.-G. Fu, X.-M. Wang, Z.-Z. Gu, Selective determination of dopamine on a boron-doped diamond electrode modified with gold nanoparticle/polyelectrolyte-coated polystyrene colloids. *Adv. Funct. Mater.* **18**(9), 1414–1421 (2008). doi:[10.1002/adfm.200701099](https://doi.org/10.1002/adfm.200701099)
31. J. Hu, X. Lu, J.S. Foord, Q. Wang, Electrochemical deposition of Pt nanoparticles on diamond substrates. *Phys. Status Solidi (a)* **206**(9), 2057–2062 (2009). doi:[10.1002/pssa.200982226](https://doi.org/10.1002/pssa.200982226)
32. J. Hu, X. Lu, J.S. Foord, Nanodiamond pretreatment for the modification of diamond electrodes by platinum nanoparticles. *Electrochem. Commun.* **12**(5), 676–679 (2010). doi:[10.1016/j.elecom.2010.03.004](https://doi.org/10.1016/j.elecom.2010.03.004)
33. S. Ferro, B.A. De, Electrocatalysis and chlorine evolution reaction at ruthenium dioxide deposited on conductive diamond. *J. Phys. Chem. B* **106**(9), 2249–2254 (2002). doi:[10.1021/jp012195i](https://doi.org/10.1021/jp012195i)
34. X. Lu, J.-P. Hu, J.S. Foord, Q. Wang, Electrochemical deposition of Pt-Ru on diamond electrodes for the electrooxidation of methanol. *J. Electroanal. Chem.* **654**(1–2), 38–43 (2011). doi:[10.1016/j.jelechem.2011.01.034](https://doi.org/10.1016/j.jelechem.2011.01.034)
35. F. Gao, N. Yang, W. Smirnov, H. Obloh, C.E. Nebel, Size-controllable and homogeneous platinum nanoparticles on diamond using wet chemically assisted electrodeposition. *Electrochim. Acta* **90**, 445–451 (2013). doi:[10.1016/j.electacta.2012.12.050](https://doi.org/10.1016/j.electacta.2012.12.050)
36. O. Enea, B. Riedo, G. Dietler, AFM study of Pt clusters electrochemically deposited onto boron-doped diamond films. *Nano Lett.* **2**(3), 241–244 (2002). doi:[10.1021/nl015666l](https://doi.org/10.1021/nl015666l)
37. C.M. Welch, M.E. Hyde, C.E. Banks, R.G. Compton, The detection of nitrate using in-situ copper nanoparticle deposition at a boron doped diamond electrode. *Anal. Sci.* **21**(12), 1421–1430 (2005). doi:[10.2116/analsci.21.1421](https://doi.org/10.2116/analsci.21.1421)
38. C.M. Welch, A.O. Simm, R.G. Compton, Oxidation of electrodeposited copper on boron doped diamond in acidic solution: manipulating the size of copper nanoparticles using voltammetry. *Electroanalysis* **18**(10), 965–970 (2006). doi:[10.1002/elan.200603493](https://doi.org/10.1002/elan.200603493)
39. I. Gonzalez-Gonzalez, F.E. Rosim, M.A. Scibioh, D.A. Tryk, M. Tague, H.D. Abruna, C.R. Cabrera, Facet-selective platinum electrodeposition at free-standing polycrystalline boron-doped diamond films. *Langmuir* **25**(17), 10329–10336 (2009). doi:[10.1021/la8035055](https://doi.org/10.1021/la8035055)
40. J. Wang, G.M. Swain, T. Tachibana, K. Kobashi, The incorporation of Pt nanoparticles into boron-doped diamond thin-films: dimensionally stable catalytic electrodes. *J. New Mater. Electrochem. Syst.* **3**(1), 75–82 (2000)

41. J.P. Hu, X. Lu, J.S. Foord, Q. Wang, Electrochemical deposition of Pt nanoparticles on diamond substrates. *Phys. Status Solidi (a)* **206**(9), 2057–2062 (2009). doi:[10.1002/pssa.200982226](https://doi.org/10.1002/pssa.200982226)
42. J. Wang, G.M. Swain, T. Tachibana, K. Kobashi, Electrocatalytic diamond thin film electrodes with incorporated Pt. *Proc. Electrochem. Soc.* **2001-2025**(Diamond Materials VII), 157–167 (2002)
43. L. Hutton, M.E. Newton, P.R. Unwin, J.V. Macpherson, Amperometric oxygen sensor based on a platinum nanoparticle-modified polycrystalline boron doped diamond disk electrode. *Anal. Chem. (Washington, DC, U. S.)* **81**(3), 1023–1032 (2009). doi:[10.1021/ac8020906](https://doi.org/10.1021/ac8020906)
44. J.A. Bennett, Y. Show, S. Wang, G.M. Swain, Pulsed galvanostatic deposition of Pt particles on microcrystalline and nanocrystalline diamond thin-film electrodes: I. characterization of as-deposited metal/diamond surfaces. *J. Electrochem. Soc.* **152**(5), E184–E192 (2005). doi:[10.1149/1.1890745](https://doi.org/10.1149/1.1890745)
45. N.R. Wilson, S.L. Clewes, M.E. Newton, P.R. Unwin, J.V. Macpherson, Impact of grain-dependent boron uptake on the electrochemical and electrical properties of polycrystalline boron doped diamond electrodes. *J. Phys. Chem. B* **110**(11), 5639–5646 (2006). doi:[10.1021/jp0547616](https://doi.org/10.1021/jp0547616)
46. K.P. Loh, S. Liang Zhao, W. De Zhang, Diamond and carbon nanotube glucose sensors based on electropolymerization. *Diam. Relat. Mater.* **13**(4–8), 1075–1079 (2004). doi:[10.1016/j.diamond.2003.11.009](https://doi.org/10.1016/j.diamond.2003.11.009)
47. P.R. Roy, M.S. Saha, T. Okajima, S.-G. Park, A. Fujishima, T. Ohsaka, Selective detection of dopamine and its metabolite, DOPAC, in the presence of ascorbic acid using diamond electrode modified by the polymer film. *Electroanalysis* **16**(21), 1777–1784 (2004). doi:[10.1002/elan.200303026](https://doi.org/10.1002/elan.200303026)
48. C.A. Martínez-Huitle, N. Suelly Fernandes, S. Ferro, A. De Battisti, M.A. Quiroz, Fabrication and application of Nafion-modified boron-doped diamond electrode as sensor for detecting caffeine. *Diam. Relat. Mater.* **19**(10), 1188–1193 (2010). doi:[10.1016/j.diamond.2010.05.004](https://doi.org/10.1016/j.diamond.2010.05.004)
49. A.O. Simm, C.E. Banks, S. Ward-Jones, T.J. Davies, N.S. Lawrence, T.G.J. Jones, L. Jiang, R.G. Compton, Boron-doped diamond microdisc arrays: electrochemical characterisation and their use as a substrate for the production of microelectrode arrays of diverse metals (Ag, Au, Cu) via electrodeposition. *Analyst* **130**(9), 1303–1311 (2005). doi:[10.1039/b506956d](https://doi.org/10.1039/b506956d)
50. C. Batchelor-McAuley, C.E. Banks, A.O. Simm, T.G.J. Jones, R.G. Compton, The electroanalytical detection of hydrazine: a comparison of the use of palladium nanoparticles supported on boron-doped diamond and palladium plated BDD microdisc array. *Analyst (Cambridge, UK)* **131**(1), 106–110 (2006). doi:[10.1039/b513751a](https://doi.org/10.1039/b513751a)
51. C. Batchelor-McAuley, C.E. Banks, A.O. Simm, T.G.J. Jones, R.G. Compton, Nano-electrochemical detection of hydrogen or protons using palladium nanoparticles: distinguishing surface and bulk hydrogen. *ChemPhysChem* **7**(5), 1081–1085 (2006). doi:[10.1002/cphc.200500571](https://doi.org/10.1002/cphc.200500571)
52. A. Salimi, M.E. Hyde, C.E. Banks, R.G. Compton, Boron doped diamond electrode modified with iridium oxide for amperometric detection of ultra trace amounts of arsenic(III). *Analyst* **129**(1), 9–14 (2004). doi:[10.1039/b312285a](https://doi.org/10.1039/b312285a)
53. N. Vinokur, B. Miller, Y. Avyigal, R. Kalish, Cathodic and anodic deposition of mercury and silver at boron-doped diamond electrodes. *J. Electrochem. Soc.* **146**(1), 125–130 (1999). doi:[10.1149/1.1391574](https://doi.org/10.1149/1.1391574)
54. I. Gonzalez-Gonzalez, D.A. Tryk, C.R. Cabrera, Polycrystalline boron-doped diamond films as supports for methanol oxidation electrocatalysts. *Diam. Relat. Mater.* **15**(2–3), 275–278 (2006). doi:[10.1016/j.diamond.2005.08.037](https://doi.org/10.1016/j.diamond.2005.08.037)
55. M. Li, G. Zhao, R. Geng, H. Hu, Facile electrocatalytic redox of hemoglobin by flower-like gold nanoparticles on boron-doped diamond surface. *Bioelectrochemical* **74**(1), 217–221 (2008). doi:[10.1016/j.bioelechem.2008.08.004](https://doi.org/10.1016/j.bioelechem.2008.08.004)

56. L.A. Hutton, M. Vidotti, A.N. Patel, M.E. Newton, P.R. Unwin, J.V. MacPherson, Electrodeposition of nickel hydroxide nanoparticles on boron-doped diamond electrodes for oxidative electrocatalysis. *J. Phys. Chem. C* **115**(5), 1649–1658 (2011). doi:[10.1021/jp109526b](https://doi.org/10.1021/jp109526b)
57. J.-S. Gao, T. Arunagiri, J.-J. Chen, P. Goodwill, O. Chyan, J. Perez, D. Golden, Preparation and characterization of metal nanoparticles on a diamond surface. *Chem. Mater.* **12**(11), 3495–3500 (2000). doi:[10.1021/cm000465o](https://doi.org/10.1021/cm000465o)
58. C. Terashima, T.N. Rao, B.V. Sarada, N. Spataru, A. Fujishima, Electrodeposition of hydrous iridium oxide on conductive diamond electrodes for catalytic sensor applications. *J. Electroanal. Chem.* **544**, 65–74 (2003). doi:[10.1016/S0022-0728\(03\)00066-4](https://doi.org/10.1016/S0022-0728(03)00066-4)
59. H. Terashima, T. Tsuji, Adsorption of bovine serum albumin onto mica surfaces studied by a direct weighing technique. *Colloid Surf. B* **27**(2–3), 115–122 (2003). doi:[10.1016/s0927-7765\(02\)00044-9](https://doi.org/10.1016/s0927-7765(02)00044-9)
60. R.B. El, G. Sine, G. Foti, C. Comninellis, A novel method for the preparation of bi-metallic (Pt-Au) nanoparticles on boron doped diamond (BDD) substrate: application to the oxygen reduction reaction. *J. Appl. Electrochem.* **37**(11), 1227–1236 (2007). doi:[10.1007/s10800-007-9359-4](https://doi.org/10.1007/s10800-007-9359-4)
61. R.B. El, G. Foti, C. Comninellis, Preparation of gold nanoparticles by heat treatment of sputter deposited gold on boron-doped diamond film electrode. *Electrochem. Commun.* **7**(4), 398–405 (2005). doi:[10.1016/j.elecom.2005.02.014](https://doi.org/10.1016/j.elecom.2005.02.014)
62. M. Limat, R.B. El, H. Jotterand, G. Foti, C. Comninellis, Electrochemical and morphological characterization of gold nanoparticles deposited on boron-doped diamond electrode. *Electrochim. Acta* **54**(9), 2410–2416 (2009). doi:[10.1016/j.electacta.2008.02.050](https://doi.org/10.1016/j.electacta.2008.02.050)
63. T.A. Ivandini, R. Sato, Y. Makide, A. Fujishima, Y. Einaga, Pt-implanted boron-doped diamond electrodes and the application for electrochemical detection of hydrogen peroxide. *Diam. Relat. Mater.* **14**(11–12), 2133–2138 (2005). doi:[10.1016/j.diamond.2005.08.022](https://doi.org/10.1016/j.diamond.2005.08.022)
64. T.A. Ivandini, R. Sato, Y. Makide, A. Fujishima, Y. Einaga, Electrochemical detection of arsenic(III) using iridium-implanted boron-doped diamond electrodes. *Anal. Chem.* **78**(18), 6291–6298 (2006). doi:[10.1021/ac0519514](https://doi.org/10.1021/ac0519514)
65. T.A. Ivandini, R. Sato, Y. Makide, A. Fujishima, Y. Einaga, Electroanalytical application of modified diamond electrodes. *Diam. Relat. Mater.* **13**(11–12), 2003–2008 (2004). doi:[10.1016/j.diamond.2004.07.004](https://doi.org/10.1016/j.diamond.2004.07.004)
66. S. Tretepvijit, A. Preechaworapun, N. Praphairaksit, U. Chuanuwatanakul, Y. Einaga, O. Chailapakul, Use of nickel implanted boron-doped diamond thin film electrode coupled to HPLC system for the determination of tetracyclines. *Talanta* **68**(4), 1329–1335 (2006). doi:[10.1016/j.talanta.2005.07.047](https://doi.org/10.1016/j.talanta.2005.07.047)
67. G.R. Salazar-Banda, K.I.B. Eguiluz, L.A. Avaca, Boron-doped diamond powder as catalyst support for fuel cell applications. *Electrochem. Commun.* **9**(1), 59–64 (2006). doi:[10.1016/j.elecom.2006.08.038](https://doi.org/10.1016/j.elecom.2006.08.038)
68. G.R. Salazar-Banda, H.B. Suffredini, L.A. Avaca, Improved stability of PtOx sol-gel-modified diamond electrodes covered with a Nafion® film. *J. Braz. Chem. Soc.* **16**(5), 903–905 (2005). doi:[10.1590/S0103-50532005000600003](https://doi.org/10.1590/S0103-50532005000600003)
69. H.B. Suffredini, G.R. Salazar-Banda, S.T. Tanimoto, M.L. Calegaro, S.A.S. Machado, L.A. Avaca, AFM studies and electrochemical characterization of boron-doped diamond surfaces modified with metal oxides by the sol-gel method. *J. Braz. Chem. Soc.* **17**(2), 257–264 (2006). doi:[10.1590/S0103-50532006000200007](https://doi.org/10.1590/S0103-50532006000200007)
70. C. Zhang, L. Gu, Y. Lin, Y. Wang, D. Fu, Z. Gu, Degradation of X-3B dye by immobilized TiO₂ photocatalysis coupling anodic oxidation on BDD electrode. *J. Photochem. Photobiol. A* **207**(1), 66–72 (2009). doi:[10.1016/j.jphotochem.2009.01.014](https://doi.org/10.1016/j.jphotochem.2009.01.014)
71. F.G. Celii, J.E. Butler, Diamond chemical vapor deposition. *Annu. Rev. Phys. Chem.* **42**, 643–684 (1991). doi:[10.1146/annurev.pc.42.100191.003235](https://doi.org/10.1146/annurev.pc.42.100191.003235)
72. J.H.T. Luong, K.B. Male, J.D. Glennon, Boron-doped diamond electrode: synthesis, characterization, functionalization and analytical applications. *Analyst (Cambridge, UK)* **134**(10), 1965–1979 (2009). doi:[10.1039/b910206j](https://doi.org/10.1039/b910206j)

73. K.B. Holt, A.J. Bard, Y. Show, G.M. Swain, Scanning electrochemical microscopy and conductive probe atomic force microscopy studies of hydrogen-terminated boron-doped diamond electrodes with different doping levels. *J. Phys. Chem. B* **108**(39), 15117–15127 (2004). doi:[10.1021/jp048222x](https://doi.org/10.1021/jp048222x)
74. G. Sine, G. Foti, C. Comninellis, Boron-doped diamond (BDD)-supported Pt/Sn nanoparticles synthesized in microemulsion systems as electrocatalysts of ethanol oxidation. *J. Electroanal. Chem.* **595**(2), 115–124 (2006). doi:[10.1016/j.jelechem.2006.07.012](https://doi.org/10.1016/j.jelechem.2006.07.012)
75. I. Yagi, T. Ishida, K. Uosaki, Electrocatalytic reduction of oxygen to water at Au nanoclusters vacuum-evaporated on boron-doped diamond in acidic solution. *Electrochem. Commun.* **6**(8), 773–779 (2004). doi:[10.1016/j.elecom.2004.05.025](https://doi.org/10.1016/j.elecom.2004.05.025)
76. S. Hrapovic, Y. Liu, J.H.T. Luong, Reusable platinum nanoparticle modified boron doped diamond microelectrodes for oxidative determination of arsenite. *Anal. Chem.* **79**(2), 500–507 (2007). doi:[10.1021/ac061528a](https://doi.org/10.1021/ac061528a)
77. Y. Zhang, V. Suryanarayanan, I. Nakazawa, S. Yoshihara, T. Shirakashi, Electrochemical behavior of Au nanoparticle deposited on as-grown and O-terminated diamond electrodes for oxygen reduction in alkaline solution. *Electrochim. Acta* **49**(28), 5235–5240 (2004). doi:[10.1016/j.electacta.2004.07.005](https://doi.org/10.1016/j.electacta.2004.07.005)
78. H. Notsu, I. Yagi, T. Tatsuma, D.A. Tryk, A. Fujishima, Introduction of oxygen-containing functional groups onto diamond electrode surfaces by oxygen plasma and anodic polarization. *Electrochem. Solid State Lett.* **2**(10), 522–524 (1999). doi:[10.1149/1.1390890](https://doi.org/10.1149/1.1390890)
79. A.O. Simm, X. Ji, C.E. Banks, M.E. Hyde, R.G. Compton, AFM studies of metal deposition: instantaneous nucleation and the growth of cobalt nanoparticles on boron-doped diamond electrodes. *ChemPhysChem* **7**(3), 704–709 (2006). doi:[10.1002/cphc.200500557](https://doi.org/10.1002/cphc.200500557)
80. D.W.M. Arrigan, Nanoelectrodes, nanoelectrode arrays, and their applications. *Analyst* **129**, 1157–1165 (2004). doi:[10.1039/B415395M](https://doi.org/10.1039/B415395M)
81. F. Maillard, M. Eikerling, O.V. Cherstiouk, S. Schreier, E. Savinova, U. Stimming, Size effects on reactivity of Pt nanoparticles in CO monolayer oxidation: the role of surface mobility. *Faraday Discuss.* **125**, 357–377 (2004). doi:[10.1039/B303911K](https://doi.org/10.1039/B303911K)
82. S.R. Belding, E.J.F. Dickinson, R.G. Compton, Diffusional cyclic voltammetry at electrodes modified with random distributions of electrocatalytic nanoparticles: theory. *J. Phys. Chem. C* **113**(25), 11149–11156 (2009). doi:[10.1021/jp901664p](https://doi.org/10.1021/jp901664p)
83. L.A. Hutton, M.E. Newton, P.R. Unwin, J.V. MacPherson, Factors controlling stripping voltammetry of lead at polycrystalline boron doped diamond electrodes: new insights from high-resolution microscopy. *Anal. Chem.* **83**(3), 735–745 (2011). doi:[10.1021/ac101626s](https://doi.org/10.1021/ac101626s)
84. S.H. Brewer, W.R. Glomm, M.C. Johnson, M.K. Knag, S. Franzen, Probing BSA binding to citrate-coated gold nanoparticles and surfaces. *Langmuir* **21**(20), 9303–9307 (2005). doi:[10.1021/la050588t](https://doi.org/10.1021/la050588t)
85. U. Griesbach, D. Zollinger, H. Putter, C. Comninellis, Evaluation of boron doped diamond electrodes for organic electrosynthesis on a preparative scale. *J. Appl. Electrochem.* **35**(12), 1265–1270 (2005). doi:[10.1007/s10800-005-9038-2](https://doi.org/10.1007/s10800-005-9038-2)
86. C. Terashima, T.N. Rao, B.V. Sarada, A. Fujishima, Electrochemical characteristics of electrodeposited iridium oxide on conductive diamond electrodes. *Chem. Sens.* **18**(Suppl. B), 106–108 (2002)
87. D.V. Bavykin, E.V. Milsom, F. Marken, D.H. Kim, D.H. Marsh, D.J. Riley, F.C. Walsh, K.H. El-Abiary, A.A. Lapkin, A novel cation-binding TiO₂ nanotube substrate for electro- and bioelectrocatalysis. *Electrochem. Commun.* **7**(10), 1050–1058 (2005). doi:[10.1016/j.elecom.2005.07.010](https://doi.org/10.1016/j.elecom.2005.07.010)
88. K.J. McKenzie, F. Marken, Electrochemical characterization of hydrous ruthenium oxide nanoparticle decorated boron-doped diamond electrodes. *ECS Solid State Lett.* **5**(9), E47–E50 (2002). doi:[10.1149/1.1497515](https://doi.org/10.1149/1.1497515)
89. M.E. Hyde, R.G. Compton, A review of the analysis of multiple nucleation with diffusion controlled growth. *J. Electroanal. Chem.* **549**(0), 1–12 (2003). doi:[http://dx.doi.org/10.1016/S0022-0728\(03\)00250-X](http://dx.doi.org/10.1016/S0022-0728(03)00250-X)

90. D. Grujicic, B. Pesic, Iron nucleation mechanisms on vitreous carbon during electrodeposition from sulfate and chloride solutions. *Electrochim. Acta* **50**(22), 4405–4418 (2005). doi:<http://dx.doi.org/10.1016/j.electacta.2005.02.013>
91. D. Grujicic, B. Pesic, Reaction and nucleation mechanisms of copper electrodeposition from ammoniacal solutions on vitreous carbon. *Electrochim. Acta* **50**(22), 4426–4443 (2005). doi:<http://dx.doi.org/10.1016/j.electacta.2005.02.012>
92. S. Jones, K. Tedsree, M. Sawangphruk, J.S. Foord, J. Fisher, D. Thompsett, S.C.E. Tsang, Promotion of direct methanol electro-oxidation by Ru terraces on Pt by using a reversed spillover mechanism. *ChemCatChem* **2**(9), 1089–1095 (2010). doi:[10.1002/cctc.201000106](https://doi.org/10.1002/cctc.201000106)
93. M.E. Hyde, R. Jacobs, R.G. Compton, In situ AFM studies of metal deposition. *J. Phys. Chem. B* **106**(43), 11075–11080 (2002). doi:[10.1021/jp0213607](https://doi.org/10.1021/jp0213607)
94. B.R. Scharifker, J. Mostany, Three-dimensional nucleation with diffusion controlled growth: Part I. Number density of active sites and nucleation rates per site. *J. Electroanal. Chem. Interf. Electrochem.* **177**(1–2), 13–23 (1984). doi:[http://dx.doi.org/10.1016/0022-0728\(84\)80207-7](http://dx.doi.org/10.1016/0022-0728(84)80207-7)
95. K.E. Toghill, G.G. Wildgoose, A. Moshar, C. Mulcahy, R.G. Compton, The fabrication and characterization of a bismuth nanoparticle modified boron doped diamond electrode and its application to the simultaneous determination of cadmium(II) and lead(II). *Electroanalysis* **20**(16), 1731–1737 (2008). doi:[10.1002/elan.200804277](https://doi.org/10.1002/elan.200804277)
96. Z.D. Wei, S.H. Chan, Electrochemical deposition of PtRu on an uncatalyzed carbon electrode for methanol electrooxidation. *J. Electroanal. Chem.* **569**(1), 23–33 (2004). doi:[10.1016/j.jelechem.2004.01.034](https://doi.org/10.1016/j.jelechem.2004.01.034)
97. N.R. Stradiotto, K.E. Toghill, L. Xiao, A. Moshar, R.G. Compton, The fabrication and characterization of a nickel nanoparticle modified boron doped diamond electrode for electrocatalysis of primary alcohol oxidation. *Electroanalysis* **21**(24), 2627–2633 (2009). doi:[10.1002/elan.200900325](https://doi.org/10.1002/elan.200900325)
98. M. Valden, X. Lai, D.W. Goodman, Onset of catalytic activity of gold clusters on titania with the appearance of nonmetallic properties. *Science* **281**(5383), 1647–1650 (1998). doi:[10.1126/science.281.5383.1647](https://doi.org/10.1126/science.281.5383.1647)
99. A. Sanchez, S. Abbet, U. Heiz, W.D. Schneider, H. Häkkinen, R.N. Barnett, U. Landman, When gold is not noble: nanoscale gold catalysts. *J. Phys. Chem. A* **103**(48), 9573–9578 (1999). doi:[10.1021/jp9935992](https://doi.org/10.1021/jp9935992)
100. M. Mavrikakis, P. Stoltze, J.K. Nørskov, Making gold less noble. *Catal. Lett.* **64**(2–4), 101–106 (2000). doi:[10.1023/A:1019028229377](https://doi.org/10.1023/A:1019028229377)
101. G. Sine, D. Smida, M. Limat, G. Foti, C. Comminellis, Microemulsion synthesized Pt/Ru/Sn nanoparticles on BDD for alcohol electro-oxidation. *J. Electrochem. Soc.* **154**(2), B170–B174 (2007). doi:[10.1149/1.2400602](https://doi.org/10.1149/1.2400602)
102. G. Sine, C. Comminellis, Nafion-assisted deposition of microemulsion-synthesized platinum nanoparticles on BDD. *Electrochim. Acta* **50**(11), 2249–2254 (2005). doi:[10.1016/j.electacta.2004.10.008](https://doi.org/10.1016/j.electacta.2004.10.008)
103. O. Niwa, Electroanalytical chemistry with carbon film electrodes and micro and nano-structured carbon film-based electrodes. *Bull. Chem. Soc. Jpn.* **78**(4), 555–571 (2005). doi:[10.1246/bcsj.78.555](https://doi.org/10.1246/bcsj.78.555)
104. J. Wang, G.M. Swain, Fabrication and evaluation of platinum/diamond composite electrodes for electrocatalysis—preliminary studies of the oxygen-reduction reaction. *J. Electrochem. Soc.* **150**(1), E24–E32 (2003). doi:[10.1149/1.1524612](https://doi.org/10.1149/1.1524612)
105. F. Montilla, E. Morallon, I. Duo, C. Comminellis, J.L. Vazquez, Platinum particles deposited on synthetic boron-doped diamond surfaces. Application to methanol oxidation. *Electrochim. Acta* **48**(25–26), 3891–3897 (2003). doi:[10.1016/s0013-4686\(03\)00526-7](https://doi.org/10.1016/s0013-4686(03)00526-7)
106. I. Duo, C. Comminellis, W. Haenni, A. Perret, Deposition of nanoparticles of iridium dioxide on a synthetic boron-doped diamond surface. *Proc. Electrochem. Soc.* **2001–2025** (Diamond Materials VII), 147–156 (2002)
107. A.J. Saterlay, S.J. Wilkins, K.B. Holt, J.S. Foord, R.G. Compton, F. Marken, Lead dioxide deposition and electrocatalysis at highly boron-doped diamond electrodes in the presence of ultrasound. *J. Electrochem. Soc.* **148**(2), E66–E72 (2001). doi:[10.1149/1.339874](https://doi.org/10.1149/1.339874)

108. X.A. Lu, J.P. Hu, J.S. Foord, Q.A. Wang, Electrochemical deposition of Pt-Ru on diamond electrodes for the electrooxidation of methanol. *J. Electroanal. Chem.* **654**(1–2), 38–43. doi:[10.1016/j.jelechem.2011.01.034](https://doi.org/10.1016/j.jelechem.2011.01.034)
109. M.E. Hyde, C.E. Banks, R.G. Compton, Anodic stripping voltammetry: an AFM study of some problems and limitations. *Electroanalysis* **16**(5), 345–354 (2004). doi:[10.1002/elan.200302863](https://doi.org/10.1002/elan.200302863)
110. N.R. Stradiotto, K.E. Toghiani, L. Xiao, A. Moshar, R.G. Compton, The fabrication and characterization of a nickel nanoparticle modified boron-doped diamond electrode for electrocatalysis of primary alcohol oxidation. *Electroanalysis* **21**(24), 2627–2633 (2009). doi:[10.1002/elan.200900325](https://doi.org/10.1002/elan.200900325)
111. F. Marken, A.S. Bhambra, D.-H. Kim, R.J. Mortimer, S.J. Stott, Electrochemical reactivity of TiO₂ nanoparticles adsorbed onto boron-doped diamond surfaces. *Electrochem. Commun.* **6** (11), 1153–1158 (2004). doi:[10.1016/j.elecom.2004.09.006](https://doi.org/10.1016/j.elecom.2004.09.006)
112. J.L. Barton, J.O.M. Bockris, The electrolytic growth of dendrites from ionic solutions. *Proc. R. Soc. A* **268**, 485–505 (1962). doi:[10.1098/rspa.1962.0154](https://doi.org/10.1098/rspa.1962.0154)
113. P. Milan, S. Mordechai, Kinetics and mechanism of electrodeposition, in *Fundamentals of Electrochemical Deposition* (Wiley, New York, 2006)
114. A. Thalhammer, R.J. Edgington, L.A. Cingolani, R. Schoepfer, R.B. Jackman, The use of nanodiamond monolayer coatings to promote the formation of functional neuronal networks. *Biomater.* **31**(8), 2097–2104 (2010). doi:<http://dx.doi.org/10.1016/j.biomaterials.2009.11.109>
115. R. Lam, M. Chen, E. Pierstorff, H. Huang, E. Osawa, D. Ho, Nanodiamond-embedded microfilm devices for localized chemotherapeutic elution. *ACS Nano* **2**(10), 2095–2102 (2008). doi:[10.1021/nm800465x](https://doi.org/10.1021/nm800465x)
116. Y. Wang, J. Zhi, Y. Liu, J. Zhang, Electrochemical detection of surfactant cetylpyridinium bromide using boron-doped diamond as electrode. *Electrochem. Commun.* **13**(1), 82–85 (2011). doi:[10.1016/j.elecom.2010.11.019](https://doi.org/10.1016/j.elecom.2010.11.019)
117. B. Guan, J. Zhi, Nanodiamond as pH-responsive vehicle for an anti-cancer drug. *Small* **6**(14), 1514–1519 (2010). doi:[10.1002/sml.200902305](https://doi.org/10.1002/sml.200902305)
118. R.S. Lewis, T. Ming, J.F. Wacker, E. Anders, E. Steel, Interstellar diamonds in meteorites. *Nature* **326**(6109) (1987). doi:[10.1038/326160a0](https://doi.org/10.1038/326160a0)
119. V. Danilenko, Shock-wave sintering of nanodiamonds. *Phys. Solid State* **46**(4), 711–715 (2004). doi:[10.1134/1.1711456](https://doi.org/10.1134/1.1711456)
120. S. Osswald, G. Yushin, V. Mochalin, S.O. Kucheyev, Y. Gogotsi, Control of sp²/sp³ carbon ratio and surface chemistry of nanodiamond powders by selective oxidation in air. *J. Am. Chem. Soc.* **128**(35), 11635–11642 (2006). doi:[10.1021/ja063303n](https://doi.org/10.1021/ja063303n)
121. A. Krueger, M. Ozawa, G. Jarre, Y. Liang, J. Stegk, L. Lu, Deagglomeration and functionalisation of detonation diamond. *Phys. Status Solidi (a)* **204**(9), 2881–2887 (2007). doi:[10.1002/pssa.200776330](https://doi.org/10.1002/pssa.200776330)
122. B. Palosz, C. Pantea, E. Grzanka, S. Stelmakh, T. Proffen, T.W. Zerda, W. Palosz, Investigation of relaxation of nanodiamond surface in real and reciprocal spaces. *Diam. Relat. Mater.* **15**(11–12), 1813–1817 (2006). doi:[10.1016/j.diamond.2006.09.001](https://doi.org/10.1016/j.diamond.2006.09.001)
123. Y. Liu, Z.N. Gu, J.L. Margrave, V.N. Khabashesku, Functionalization of nanoscale diamond powder: fluoro-, alkyl-, amino-, and amino acid-nanodiamond derivatives. *Chem. Mater.* **16** (20), 3924–3930 (2004). doi:[10.1021/cm048875q](https://doi.org/10.1021/cm048875q)
124. I. Kulakova, Surface chemistry of nanodiamonds. *Phys. Solid State* **46**(4), 636–643 (2004)
125. A. Hartl, E. Schmich, J.A. Garrido, J. Hernando, S.C.R. Catharino, S. Walter, P. Feulner, A. Kromka, D. Steinmuller, M. Stutzmann, Protein-modified nanocrystalline diamond thin films for biosensor applications. *Nat. Mater.* **3**(10), 736–742 (2004). doi:http://www.nature.com/nmat/journal/v3/n10/supinfo/nmat1204_S1.html
126. F. Neugart, A. Zappe, F. Jelezko, C. Tietz, J.P. Boudou, A. Krueger, J. Wrachtrup, Dynamics of diamond nanoparticles in solution and cells. *Nano Lett.* **7**(12), 3588–3591 (2007). doi:[10.1021/nl0716303](https://doi.org/10.1021/nl0716303)
127. P.H. Chung, E. Perevedentseva, C.L. Cheng, The particle size-dependent photoluminescence of nanodiamonds. *Surf. Sci.* **601**(18), 3866–3870 (2007). doi:[10.1016/j.susc.2007.04.150](https://doi.org/10.1016/j.susc.2007.04.150)

128. O.A. Williams, J. Hees, C. Dieker, W. Jager, L. Kirste, C.E. Nebel, Size-dependent reactivity of diamond nanoparticles. *ACS Nano* **4**(8), 4824–4830 (2010). doi:[10.1021/nn100748k](https://doi.org/10.1021/nn100748k)
129. V.S. Bondar, I.O. Pozdnyakova, A.P. Puzyr, Applications of nanodiamonds for separation and purification of proteins. *Phys. Solid State* **46**(4), 758–760 (2004). doi:[10.1134/1.1711468](https://doi.org/10.1134/1.1711468)
130. D. Shin, H. Watanabe, C.E. Nebel, Insulator–metal transition of intrinsic diamond. *J. Am. Chem. Soc.* **127**(32), 11236–11237 (2005). doi:[10.1021/ja052834t](https://doi.org/10.1021/ja052834t)
131. C.E. Nebel, H. Kato, B. Rezek, D. Shin, D. Takeuchi, H. Watanabe, T. Yamamoto, Electrochemical properties of undoped hydrogen terminated CVD diamond. *Diam. Relat. Mater.* **15**(2–3), 264–268 (2006). doi:<http://dx.doi.org/10.1016/j.diamond.2005.08.012>
132. V. Chakrapani, J.C. Angus, A.B. Anderson, S.D. Wolter, B.R. Stoner, G.U. Sumanasekera, Charge transfer equilibria between diamond and an aqueous oxygen electrochemical redox couple. *Science* **318**(5855), 1424–1430 (2007). doi:[10.1126/science.1148841](https://doi.org/10.1126/science.1148841)
133. K.B. Holt, D.J. Caruana, E.J. Millan-Barrios, Electrochemistry of undoped diamond nanoparticles: accessing surface redox states. *J. Am. Chem. Soc.* **131**(32), 11272–11273 (2009). doi:[10.1021/ja902216n](https://doi.org/10.1021/ja902216n)
134. T. Bruelle, A. Denisenko, H. Sternschulte, U. Stimming, Catalytic activity of platinum nanoparticles on highly boron-doped and 100-oriented epitaxial diamond towards HER and HOR. *Phys. Chem. Chem. Phys.* **13**(28), 12883–12891 (2011). doi:[10.1039/c1cp20852g](https://doi.org/10.1039/c1cp20852g)
135. A.S. Barnard, M. Sternberg, Crystallinity and surface electrostatics of diamond nanocrystals. *J. Mater. Chem.* **17**(45), 4811–4819 (2007). doi:[10.1039/b710189a](https://doi.org/10.1039/b710189a)
136. J. Zang, Y. Wang, L. Bian, J. Zhang, F. Meng, Y. Zhao, S. Ren, X. Qu, Surface modification and electrochemical behaviour of undoped nanodiamonds. *Electrochim. Acta* **72**, 68–73 (2012). doi:[10.1016/j.electacta.2012.03.169](https://doi.org/10.1016/j.electacta.2012.03.169)
137. L. Wang, Y. Gao, Q. Xue, H. Liu, T. Xu, Effects of nano-diamond particles on the structure and tribological property of Ni-matrix nanocomposite coatings. *Mater. Sci. Eng. A* **A390** (1–2), 313–318 (2005). doi:[10.1016/j.msea.2004.08.033](https://doi.org/10.1016/j.msea.2004.08.033)
138. L. La-Torre-Riveros, K. Soto, M.A. Scibioh, C.R. Cabrera, Electrophoretically fabricated diamond nanoparticle-based electrodes. *J. Electrochem. Soc.* **157**(6), B831–B836 (2010). doi:[10.1149/1.3374403](https://doi.org/10.1149/1.3374403)
139. X.Y. Zhao, J.B. Zang, Y.H. Wang, L.Y. Bian, J.K. Yu, Electropolymerizing polyaniline on undoped 100 nm diamond powder and its electrochemical characteristics. *Electrochem. Commun.* **11**(6), 1297–1300 (2009). doi:[10.1016/j.elecom.2009.04.029](https://doi.org/10.1016/j.elecom.2009.04.029)
140. J. Zang, Y. Wang, X. Zhao, G. Xin, S. Sun, X. Qu, S. Ren, Electrochemical synthesis of polyaniline on nanodiamond powder. *Int. J. Electrochem. Sci.* **7**(2), 1677–1687 (2012)
141. E. Tamburri, S. Orlanducci, V. Guglielmotti, G. Reina, M. Rossi, M.L. Terranova, Engineering detonation nanodiamond–polyaniline composites by electrochemical routes: structural features and functional characterizations. *Polymer* **52**(22), 5001–5008 (2011). doi:[10.1016/j.polymer.2011.09.003](https://doi.org/10.1016/j.polymer.2011.09.003)
142. E. Tamburri, V. Guglielmotti, S. Orlanducci, M.L. Terranova, D. Sordi, D. Passeri, R. Matassa, M. Rossi, Nanodiamond-mediated crystallization in fibers of PANI nanocomposites produced by template-free polymerization: conductive and thermal properties of the fibrillar networks. *Polymer* **53**(19), 4045–4053 (2012). doi:[10.1016/j.polymer.2012.07.014](https://doi.org/10.1016/j.polymer.2012.07.014)
143. H. Zhuang, B. Song, T. Staedler, X. Jiang, Microcontact printing of monodiamond nanoparticles: an effective route to patterned diamond structure fabrication. *Langmuir* **27**(19), 11981–11989 (2011). doi:[10.1021/la2024428](https://doi.org/10.1021/la2024428)
144. W. Hongthani, D.J. Fermin, Layer-by-layer assembly and redox properties of undoped HPHT diamond particles. *Diam. Relat. Mater.* **19**(7–9), 680–684 (2010). doi:[10.1016/j.diamond.2010.01.039](https://doi.org/10.1016/j.diamond.2010.01.039)
145. G.L. Bilbro, Theory of electrodeposition of diamond nanoparticles. *Diam. Relat. Mater.* **11** (8), 1572–1577 (2002). doi:[10.1016/S0925-9635\(02\)00104-8](https://doi.org/10.1016/S0925-9635(02)00104-8)
146. L.-N. Tsai, G.-R. Shen, Y.-T. Cheng, W. Hsu, Performance improvement of an electrothermal microactuator fabricated using Ni-diamond nanocomposite. *J. Microelectromech. Syst.* **15**(1), 149–158 (2006). doi:[10.1109/JMEMS.2005.863737](https://doi.org/10.1109/JMEMS.2005.863737)

147. E.A. Levashov, P.V. Vakaev, E.I. Zamulaeva, A.E. Kudryashov, V.V. Kurbatkin, D.V. Shtansky, A.A. Voevodin, A. Sanz, Disperse-strengthening by nanoparticles advanced tribological coatings and electrode materials for their deposition. *Surf. Coat. Technol.* **201** (13), 6176–6181 (2007). doi:[10.1016/j.surfcoat.2006.08.134](https://doi.org/10.1016/j.surfcoat.2006.08.134)
148. T. Fujimura, V.Y. Dolmatov, G.K. Burkat, E.A. Orlova, M.V. Veretennikova, Electrochemical codeposition of Sn-Pb-metal alloy along with detonation synthesis nanodiamonds. *Diam. Relat. Mater.* **13**(11–12), 2226–2229 (2004). doi:[10.1016/j.diamond.2004.06.009](https://doi.org/10.1016/j.diamond.2004.06.009)
149. L.Y. Bian, Y.H. Wang, J. Lu, J.B. Zang, Synthesis and electrochemical properties of TiO₂/nanodiamond nanocomposite. *Diam. Relat. Mater.* **19**(10), 1178–1182 (2010). doi:[10.1016/j.diamond.2010.05.007](https://doi.org/10.1016/j.diamond.2010.05.007)
150. L.Y. Bian, Y.H. Wang, J.B. Zang, F.W. Meng, Y.L. Zhao, Detonation-synthesized nanodiamond as a stable support of Pt electrocatalyst for methanol electrooxidation. *Int. J. Electrochem. Sci.* **7**(8), 7295–7303 (2012)
151. L. La-Torre-Riveros, R. Guzman-Blas, A.E. Mendez-Torres, M. Prelas, D.A. Tryk, C.R. Cabrera, Diamond nanoparticles as a support for Pt and Pt-Ru catalysts for direct methanol fuel cells. *ACS Appl. Mater. Interfaces* **4**(2), 1134–1147 (2012). doi:[10.1021/am2018628](https://doi.org/10.1021/am2018628)
152. L. La-Torre-Riveros, E. Abel-Tatis, A.E. Mendez-Torres, D.A. Tryk, M. Prelas, C.R. Cabrera, Synthesis of platinum and platinum-ruthenium-modified diamond nanoparticles. *J. Nanopart. Res.* **13**(7), 2997–3009 (2011). doi:[10.1007/s11051-010-0196-8](https://doi.org/10.1007/s11051-010-0196-8)
153. L. Cunci, C.R. Cabrera, Preparation and electrochemistry of boron-doped diamond nanoparticles on glassy carbon electrodes. *Electrochem. Solid State Lett.* **14**(3), K17–K19 (2011). doi:[10.1149/1.3532943](https://doi.org/10.1149/1.3532943)
154. J. Scholz, A.J. McQuillan, K.B. Holt, Redox transformations at nanodiamond surfaces revealed by in situ infrared spectroscopy. *Chem. Commun.* **47**(44), 12140–12142 (2011). doi:[10.1039/C1CC14961J](https://doi.org/10.1039/C1CC14961J)
155. D. Plana, J.J.L. Humphrey, K.A. Bradley, V. Celorrio, D.J. Fermin, Charge transport across high surface area metal/diamond nanostructured composites. *ACS Appl. Mater. Interf.* **5**(8), 2985–2990 (2013). doi:[10.1021/am302397p](https://doi.org/10.1021/am302397p)
156. T. Kondo, K. Hirata, T. Kawai, M. Yuasa, Self-assembled fabrication of a polycrystalline boron-doped diamond surface supporting Pt (or Pd)/Au-shell/core nanoparticles on the (111) facets and Au nanoparticles on the (100) facets. *Diam. Relat. Mater.* **20**(8), 1171–1178 (2011). doi:<http://dx.doi.org/10.1016/j.diamond.2011.06.033>
157. V.A. Plotnikov, B.F. Dem'yanov, S.V. Makarov, Effects of aluminum on the interaction of detonation diamond nanocrystals during high-temperature annealing. *Tech. Phys. Lett.* **35**(5), 473–475 (2009). doi:[10.1134/S1063785009050265](https://doi.org/10.1134/S1063785009050265)
158. K.E. Toghiani, L. Xiao, N.R. Stradiotto, R.G. Compton, The determination of methanol using an electrolytically fabricated nickel microparticle modified boron doped diamond electrode. *Electroanalysis* **22**(5), 491–500 (2010). doi:[10.1002/elan.200900523](https://doi.org/10.1002/elan.200900523)
159. A.M. Panich, A. Altman, A.I. Shames, V.Y. Osipov, A.E. Aleksenskiy, A.Y. Vul, Proton magnetic resonance study of diamond nanoparticles decorated by transition metal ions. *J. Phys. D Appl. Phys.* **44**(12), 125303 (2011). doi:[10.1088/0022-3727/44/12/125303](https://doi.org/10.1088/0022-3727/44/12/125303)
160. A.M. Panich, A.I. Shames, O. Medvedev, V.Y. Osipov, A.E. Aleksenskiy, A.Y. Vul', Magnetic resonance study of detonation nanodiamonds with surface chemically modified by transition metal ions. *Appl. Magn. Reson.* **36**(2–4), 317–329 (2009). doi:[10.1007/s00723-009-0028-0](https://doi.org/10.1007/s00723-009-0028-0)
161. H.J. Looi, L.Y.S. Pang, M.D. Whitfield, J.S. Foord, R.B. Jackman, Engineering low resistance contacts on p-type hydrogenated diamond surfaces. *Diam. Relat. Mater.* **9**(3–6), 975–981 (2000). doi:[http://dx.doi.org/10.1016/S0925-9635\(00\)00240-5](http://dx.doi.org/10.1016/S0925-9635(00)00240-5)
162. Y. Jia, W. Zhu, E.G. Wang, Y. Huo, Z. Zhang, Initial stages of Ti growth on diamond (100) surfaces: from single adatom diffusion to quantum wire formation. *Phys. Rev. Lett.* **94**(8), 086101 (2005). doi:[10.1103/PhysRevLett.94.086101](https://doi.org/10.1103/PhysRevLett.94.086101)

163. S. Stehlik, T. Petit, H.A. Girard, J.-C. Arnault, A. Kromka, B. Rezek, Nanoparticles assume electrical potential according to substrate, size, and surface termination. *Langmuir* **29**(5), 1634–1641 (2013). doi:[10.1021/la304472w](https://doi.org/10.1021/la304472w)
164. I. Motochi, N.W. Makau, G.O. Amolo, Metal–semiconductor ohmic contacts: an ab initio density functional theory study of the structural and electronic properties of metal–diamond (111)-(1x1) interfaces. *Diam. Relat. Mater.* **23** 10–17 (2012). doi:<http://dx.doi.org/10.1016/j.diamond.2011.12.021>
165. M.W. Geis, J.C. Twichell, T.M. Lyszczarz, Diamond emitters fabrication and theory. *J. Vac. Sci. Technol. B* **14**(3), 2060–2067 (1996). doi:[10.1116/1.588986](https://doi.org/10.1116/1.588986)
166. T. Tyler, V.V. Zhirnov, A.V. Kvit, D. Kang, J.J. Hren, Electron emission from diamond nanoparticles on metal tips. *Appl. Phys. Lett.* **82**(17), 2904–2906 (2003). doi:[10.1063/1.1570498](https://doi.org/10.1063/1.1570498)
167. N.S. Xu, Y. Tzeng, R.V. Latham, Similarities in the ‘cold’ electron emission characteristics of diamond coated molybdenum electrodes and polished bulk graphite surfaces. *J. Phys. D Appl. Phys.* **26**(10), 1776 (1993). doi:[10.1088/0022-3727/26/10/035](https://doi.org/10.1088/0022-3727/26/10/035)
168. V.V. Zhirnov, E.I. Givargizov, P.S. Plekhanov, Field emission from silicon spikes with diamond coatings. *J. Vac. Sci. Technol. B* **13**(2), 418–421 (1995). doi:[10.1116/1.587960](https://doi.org/10.1116/1.587960)
169. A.V. Karabutov, V.D. Frolov, V.I. Konov, Diamond/sp²-bonded carbon structures: quantum well field electron emission? *Diam. Relat. Mater.* **10**(3–7), 840–846 (2001). doi:[http://dx.doi.org/10.1016/S0925-9635\(00\)00569-0](http://dx.doi.org/10.1016/S0925-9635(00)00569-0)
170. Y. Takasu, S. Konishi, W. Sugimoto, Y. Murakami, Catalytic formation of nanochannels in the surface layers of diamonds by metal nanoparticles. *Electrochem. Solid State Lett.* **9**(7), C114–C117 (2006). doi:[10.1149/1.2201995](https://doi.org/10.1149/1.2201995)
171. T. Brulle, A. Denisenko, H. Sternschulte, U. Stimming, Catalytic activity of platinum nanoparticles on highly boron-doped and 100-oriented epitaxial diamond towards HER and HOR. *Phys. Chem. Chem. Phys.* **13**(28), 12883–12891 (2011). doi:[10.1039/C1CP20852G](https://doi.org/10.1039/C1CP20852G)
172. I. Casella, M. Contursi, Cobalt oxide electrodeposition on various electrode substrates from alkaline medium containing Co–gluconate complexes: a comparative voltammetric study. *J. Solid State Electrochem.* **16**(12), 3739–3746 (2012). doi:[10.1007/s10008-012-1794-4](https://doi.org/10.1007/s10008-012-1794-4)
173. S.A. Yao, R.E. Ruther, L. Zhang, R.A. Franking, R.J. Hamers, J.F. Berry, Covalent attachment of catalyst molecules to conductive diamond: CO₂ reduction using “smart” electrodes. *J. Am. Chem. Soc.* **134**(38), 15632–15635 (2012). doi:[10.1021/ja304783j](https://doi.org/10.1021/ja304783j)
174. I. Zegkinoglou, P.L. Cook, P.S. Johnson, W. Yang, J. Guo, D. Pickup, R. González-Moreno, C. Rogero, R.E. Ruther, M.L. Rigsby, J.E. Ortega, R.J. Hamers, F.J. Himpsel, Electronic structure of diamond surfaces functionalized by Ru(tpy)₂. *J. Phys. Chem. C* **116**(26), 13877–13883 (2012). doi:[10.1021/jp304016t](https://doi.org/10.1021/jp304016t)
175. P. Wang, M. Cao, Y. Ao, C. Wang, J. Hou, J. Qian, Investigation on Ce-doped TiO₂-coated BDD composite electrode with high photoelectrocatalytic activity under visible light irradiation. *Electrochem. Commun.* **13**(12), 1423–1426 (2011). doi:[10.1016/j.elecom.2011.09.009](https://doi.org/10.1016/j.elecom.2011.09.009)
176. T. Ochiai, K. Nakata, T. Murakami, A. Fujishima, Y. Yao, D.A. Tryk, Y. Kubota, Development of solar-driven electrochemical and photocatalytic water treatment system using a boron-doped diamond electrode and TiO₂ photocatalyst. *Water Res.* **44**(3), 904–910 (2010). doi:[10.1016/j.watres.2009.09.060](https://doi.org/10.1016/j.watres.2009.09.060)
177. T. Zhao, J. Wang, L. Jiang, T. Cheng, Method for manufacturing titania and boron-doped diamond (BDD) composite photoelectrocatalytic synergistic electrode. CN101875007A
178. J.T. Matsushima, A.B. Couto, N.G. Ferreira, M.R. Baldan, Study of the electrochemical deposition of Cu/Sn alloy nanoparticles on boron doped diamond films for electrocatalytic nitrate reduction. *MRS Online Proc. Libr.* **1511** (Diamond Electronics and Biotechnology), opl.2013.2016, 2016 pp. (2012). doi:[10.1557/opl.2013.16](https://doi.org/10.1557/opl.2013.16)
179. M.-J. Song, J.-H. Kim, S.-K. Lee, D.-S. Lim, Fabrication of Pt nanoparticles-decorated CVD diamond electrode for biosensor applications. *Anal. Sci.* **27**(10), 985–989 (2011). doi:[10.2116/analsci.27.985](https://doi.org/10.2116/analsci.27.985)

180. L.Y. Bian, Y.H. Wang, J.B. Zang, J.K. Yu, H. Huang, Electrodeposition of Pt nanoparticles on undoped nanodiamond powder for methanol oxidation electrocatalysts. *J. Electroanal. Chem.* **644**(1), 85–88 (2010). doi:[10.1016/j.jelechem.2010.04.001](https://doi.org/10.1016/j.jelechem.2010.04.001)
181. N. Yang, F. Gao, C.E. Nebel, Diamond decorated with copper nanoparticles for electrochemical reduction of carbon dioxide. *Anal. Chem.* **85**(12), 5764–5769 (2013). doi:[10.1021/ac400377y](https://doi.org/10.1021/ac400377y)
182. L. La-Torre-Riveros, E. Abel-Tatis, A.E. Méndez-Torres, D.A. Tryk, M. Prelas, C.R. Cabrera, Synthesis of platinum and platinum-ruthenium-modified diamond nanoparticles. *J. Nanopart. Res.* **13**(7), 2997–3009 (2011). doi:[10.1007/s11051-010-0196-8](https://doi.org/10.1007/s11051-010-0196-8)
183. P. Kim, J.B. Joo, W. Kim, J. Kim, I.K. Song, J. Yi, NaBH₄-assisted ethylene glycol reduction for preparation of carbon-supported Pt catalyst for methanol electro-oxidation. *J. Power Sources* **160**(2), 987–990 (2006). doi:[10.1016/j.jpowsour.2006.02.050](https://doi.org/10.1016/j.jpowsour.2006.02.050)
184. Y. Liu, Z. Gu, J.L. Margrave, V.N. Khabashesku, Functionalization of nanoscale diamond powder: fluoro-, alkyl-, amino-, and amino acid-nanodiamond derivatives. *Chem. Mater.* **16**(20), 3924–3930 (2004). doi:[10.1021/cm048875q](https://doi.org/10.1021/cm048875q)
185. A. Barras, S. Szunerits, L. Marcon, N. Monfilliette-Dupont, R. Boukherroub, Functionalization of diamond nanoparticles using “click” chemistry. *Langmuir* **26**(16), 13168–13172 (2010). doi:[10.1021/la101709q](https://doi.org/10.1021/la101709q)
186. A. Krueger, D. Lang, Functionality is key: recent progress in the surface modification of nanodiamond. *Adv. Func. Mater.* **22**(5), 890–906 (2012). doi:[10.1002/adfm.201102670](https://doi.org/10.1002/adfm.201102670)
187. C.-M. Sung, Diamond neural devices and associated methods. US20110282421A1
188. A. Thalhammer, R.J. Edgington, L.A. Cingolani, R. Schoepfer, R.B. Jackman, The use of nanodiamond monolayer coatings to promote the formation of functional neuronal networks. *Biomaterials.* **31**(8), 2097–2104 (2010). doi:[10.1016/j.biomaterials.2009.11.109](https://doi.org/10.1016/j.biomaterials.2009.11.109)
189. N. Yang, R. Hoffmann, W. Smirnov, C.E. Nebel, Interface properties of cytochrome c on a nano-textured diamond surface. *Diam. Relat. Mater.* **20**(2), 269–273 (2011). doi:[10.1016/j.diamond.2010.12.012](https://doi.org/10.1016/j.diamond.2010.12.012)
190. N. Yang, W. Smirnov, A. Kriele, R. Hoffmann, C.E. Nebel, Diamond nanotextured surfaces for enhanced protein redox activity. *Phys. Status Solidi (a)* **207**(9), 2069–2072 (2010). doi:[10.1002/pssa.201000085](https://doi.org/10.1002/pssa.201000085)
191. B.C. Janegitz, R.A. Medeiros, R.C. Rocha-Filho, O. Fatibello-Filho, Direct electrochemistry of tyrosinase and biosensing for phenol based on gold nanoparticles electrodeposited on a boron-doped diamond electrode. *Diam. Relat. Mater.* **25**, 128–133 (2012). doi:[10.1016/j.diamond.2012.02.023](https://doi.org/10.1016/j.diamond.2012.02.023)
192. A. Liu, Q. Ren, T. Xu, M. Yuan, W. Tang, Morphology-controllable gold nanostructures on phosphorus doped diamond-like carbon surfaces and their electrocatalysis for glucose oxidation. *Sens. Actuators B* **162**(1), 135–142 (2012). doi:[10.1016/j.snb.2011.12.050](https://doi.org/10.1016/j.snb.2011.12.050)
193. M.-J. Song, S.-K. Lee, J.-H. Kim, D.-S. Lim, Dopamine sensor based on a boron-doped diamond electrode modified with a polyaniline/Au nanocomposites in the presence of ascorbic acid. *Anal. Sci.* **28**(6), 583–587 (2012). doi:[10.2116/analsci.28.583](https://doi.org/10.2116/analsci.28.583)
194. Y. Yu, Y. Zhou, L. Wu, J. Zhi, Electrochemical biosensor based on boron-doped diamond electrodes with modified surfaces. *Int. J. Electrochem.* **2012**, (2012). doi:[10.1155/2012/567171](https://doi.org/10.1155/2012/567171)
195. B. Liu, J. Hu, J.S. Foord, Electrochemical detection of DNA hybridization by a zirconia modified diamond electrode. *Electrochem. Commun.* **19**, 46–49 (2012). doi:[10.1016/j.elecom.2012.03.007](https://doi.org/10.1016/j.elecom.2012.03.007)
196. A. Zeng, C. Jin, S.-J. Cho, H.O. Seo, Y.D. Kim, D.C. Lim, D.H. Kim, B. Hong, J.-H. Boo, Nickel nano-particle modified nitrogen-doped amorphous hydrogenated diamond-like carbon film for glucose sensing. *Mater. Res. Bull.* **47**(10), 2713–2716 (2012). doi:[10.1016/j.materresbull.2012.04.041](https://doi.org/10.1016/j.materresbull.2012.04.041)
197. W. Wu, R. Xie, L. Bai, Z. Tang, Z. Gu, Direct electrochemistry of *Shewanella loihica* PV-4 on gold nanoparticles-modified boron-doped diamond electrodes fabricated by layer-by-layer technique. *J. Nanosci. Nanotechnol.* **12**(5), 3903–3908 (2012). doi:[10.1166/jnn.2012.6175](https://doi.org/10.1166/jnn.2012.6175)

198. C.-C. Wu, C.-C. Han, H.-C. Chang, Applications of surface-functionalized diamond nanoparticles for mass-spectrometry-based proteomics. *J. Chin. Chem. Soc.* **57**(3B), 583–594 (2010). doi:[10.1002/jccs.201000082](https://doi.org/10.1002/jccs.201000082)
199. X. Fuku, F. Iftikar, E. Hess, E. Iwuoha, P. Baker, Cytochrome c biosensor for determination of trace levels of cyanide and arsenic compounds. *Anal. Chim. Acta* **730**, 49–59 (2012). doi:[10.1016/j.aca.2012.02.025](https://doi.org/10.1016/j.aca.2012.02.025)
200. R. Hoffmann, A. Kriele, S. Kopta, W. Smirnov, N. Yang, C.E. Nebel, Adsorption of cytochrome c on diamond. *Physica Status Solidi (a)* **207**(9), 2073–2077 (2010). doi:[10.1002/pssa.201000043](https://doi.org/10.1002/pssa.201000043)
201. A. Rahim Ruslinda, K. Tanabe, S. Ibori, X. Wang, H. Kawarada, Effects of diamond-FET-based RNA aptamer sensing for detection of real sample of HIV-1 Tat protein. *Biosens. Bioelectron.* **40**(1), 277–282 (2013). doi:<http://dx.doi.org/10.1016/j.bios.2012.07.048>
202. M.-J. Song, S.-K. Lee, J.-Y. Lee, J.-H. Kim, D.-S. Lim, Electrochemical sensor based on Au nanoparticles decorated boron-doped diamond electrode using ferrocene-tagged aptamer for proton detection. *J. Electroanal. Chem.* **677–680**, 139–144 (2012). doi:[10.1016/j.jelechem.2012.05.019](https://doi.org/10.1016/j.jelechem.2012.05.019)
203. D.T. Tran, V. Vermeeren, L. Grieten, S. Wenmackers, P. Wagner, J. Pollet, K.P.F. Janssen, L. Michiels, J. Lammertyn, Nanocrystalline diamond impedimetric aptasensor for the label-free detection of human IgE. *Biosens. Bioelectron.* **26**(6), 2987–2993 (2011). doi:[10.1016/j.bios.2010.11.053](https://doi.org/10.1016/j.bios.2010.11.053)
204. X. Fuku, F. Iftikar, E. Hess, E. Iwuoha, P. Baker, Cytochrome c biosensor for determination of trace levels of cyanide and arsenic compounds. *Anal. Chim. Acta* **730**(0), 49–59 (2012). doi:<http://dx.doi.org/10.1016/j.aca.2012.02.025>
205. A. Kriele, O.A. Williams, M. Wolfer, J.J. Hees, W. Smirnov, C.E. Nebel, Formation of nanopores in nano-crystalline diamond films. *Chem. Phys. Lett.* **507**(4–6), 253–259 (2011). doi:[10.1016/j.cplett.2011.03.089](https://doi.org/10.1016/j.cplett.2011.03.089)
206. F. Weigl, S. Fricker, H.-G. Boyen, C. Dietrich, B. Koslowski, A. Plettl, O. Pursche, P. Ziemann, P. Walther, C. Hartmann, M. Ott, M. Moeller, From self-organized masks to nanotips: a new concept for the preparation of densely packed arrays of diamond field emitters. *Diam. Relat. Mater.* **15**(10), 1689–1694 (2006). doi:[10.1016/j.diamond.2006.02.007](https://doi.org/10.1016/j.diamond.2006.02.007)
207. K. Honda, M. Yoshimura, T.N. Rao, D.A. Tryk, A. Fujishima, K. Yasui, Y. Sakamoto, K. Nishio, H. Masuda, Electrochemical properties of Pt-modified nano-honeycomb diamond electrodes. *J. Electroanal. Chem.* **514**(1–2), 35–50 (2001). doi:[10.1016/S0022-0728\(01\)00614-3](https://doi.org/10.1016/S0022-0728(01)00614-3)
208. O. Babchenko, E. Verveniotis, K. Hruska, M. Ledinsky, A. Kromka, B. Rezek, Direct growth of sub-micron diamond structures. *Vacuum* **86**(6), 693–695 (2012). doi:[10.1016/j.vacuum.2011.08.011](https://doi.org/10.1016/j.vacuum.2011.08.011)
209. N. Yang, W. Smirnov, C.E. Nebel, Three-dimensional electrochemical reactions on tip-coated diamond nanowires with nickel nanoparticles. *Electrochem. Commun.* **27**, 89–91 (2013). doi:[10.1016/j.elecom.2012.10.044](https://doi.org/10.1016/j.elecom.2012.10.044)
210. C.E. Nebel, N. Yang, H. Uetsuka, E. Osawa, N. Tokuda, O. Williams, Diamond nano-wires, a new approach towards next generation electrochemical gene sensor platforms. *Diam. Relat. Mater.* **18**(5–8), 910–917 (2009). doi:[10.1016/j.diamond.2008.11.024](https://doi.org/10.1016/j.diamond.2008.11.024)
211. P. Subramanian, Y. Coffinier, D. Steinmuller-Nethl, J. Foord, R. Boukherroub, S. Szunerits, Diamond nanowires decorated with metallic nanoparticles: a novel electrical interface for the immobilization of histidinylated biomolecules. *Electrochim. Acta*, Ahead of Print (2012). doi:[10.1016/j.electacta.2012.11.010](https://doi.org/10.1016/j.electacta.2012.11.010)
212. M. Wei, C. Terashima, M. Lv, A. Fujishima, Z.-Z. Gu, Boron-doped diamond nanoglass array for electrochemical sensors. *Chem. Commun.* **24**, 3624–3626 (2009). doi:[10.1039/B903284C](https://doi.org/10.1039/B903284C)
213. D.H. Wang, L.-S. Tan, H. Huang, L. Dai, E. Osawa, In-situ nanocomposite synthesis: arylcarbonylation and grafting of primary diamond nanoparticles with a poly(ether-ketone) in polyphosphoric acid. *Macromolecules* **42**(1), 114–124 (2009). doi:[10.1021/ma8019078](https://doi.org/10.1021/ma8019078)

214. H.A. Girard, S. Perruchas, C. Gesset, M. Chaigneau, L. Vieille, J.-C. Arnault, P. Bergonzo, J.-P. Boilot, T. Gacoin, Electrostatic grafting of diamond nanoparticles: a versatile route to nanocrystalline diamond thin films. *ACS Appl. Mater. Interf.* **1**(12), 2738–2746 (2009). doi:[10.1021/am900458g](https://doi.org/10.1021/am900458g)
215. O. Babchenko, A. Kromka, K. Hruska, M. Michalka, J. Potmesil, M. Vanecek, Nanostructuring of diamond films using self-assembled nanoparticles. *Cent. Eur. J. Phys.* **7**(2), 310–314 (2009). doi:[10.2478/s11534-009-0026-8](https://doi.org/10.2478/s11534-009-0026-8)
216. G.A. Powch, A.R. Jain, Directed self assembly: a novel, high speed method of nanocoating ultra-thin films and monolayers of particles. NSTI Nanotechnology Conference and Expo, NSTI-Nanotech 2012 (Santa Clara, CA, USA), pp. 474–477 (2012). CRC Press. ISBN: 978-1-4665-6275-2
217. H. Sim, S.-I. Hong, S.-K. Lee, D.-S. Lim, J.-E. Jin, S.-W. Hwang, Fabrication of boron-doped nanocrystalline diamond nanoflowers based on 3D Cu(OH)₂ dendritic architectures. *J. Korean Phys. Soc.* **60**(5), 836–841 (2012). doi:[10.3938/jkps.60.836](https://doi.org/10.3938/jkps.60.836)
218. D. Yamada, T.A. Ivandini, M. Komatsu, A. Fujishima, Y. Einaga, Anodic stripping voltammetry of inorganic species of As³⁺ and As⁵⁺ at gold-modified boron doped diamond electrodes. *J. Electroanal. Chem.* **615**(2), 145–153 (2008). doi:[10.1016/j.jelechem.2007.12.004](https://doi.org/10.1016/j.jelechem.2007.12.004)
219. G. Sine, I. Duo, R.B. El, G. Foti, C. Comninellis, Deposition of clusters and nanoparticles onto boron-doped diamond electrodes for electrocatalysis. *J. Appl. Electrochem.* **36**(8), 847–862 (2006). doi:[10.1007/s10800-006-9159-2](https://doi.org/10.1007/s10800-006-9159-2)
220. K.E. Toghill, L. Xiao, G.G. Wildgoose, R.G. Compton, Electroanalytical determination of cadmium(II) and lead(II) using an antimony nanoparticle modified boron-doped diamond electrode. *Electroanalysis* **21**(10), 1113–1118 (2009). doi:[10.1002/elan.200904547](https://doi.org/10.1002/elan.200904547)
221. T.-L. Wee, B.D. Sherman, D. Gust, A.L. Moore, T.A. Moore, Y. Liu, J.C. Scaiano, Photochemical synthesis of a water oxidation catalyst based on cobalt nanostructures. *J. Am. Chem. Soc.* **133**(42), 16742–16745 (2011). doi:[10.1021/ja206280g](https://doi.org/10.1021/ja206280g)
222. V. Saez, J. Gonzalez-Garcia, F. Marken, Active catalysts of sonoelectrochemically prepared iron metal nanoparticles for the electroreduction of chloroacetates. *Phys. Procedia* **3**(1), 105–109 (2010). doi:[10.1016/j.phpro.2010.01.015](https://doi.org/10.1016/j.phpro.2010.01.015)
223. L. Rassaei, M. Sillanpaa, R.W. French, R.G. Compton, F. Marken, Arsenite determination in phosphate media at electroaggregated gold nanoparticle deposits. *Electroanalysis* **20**(12), 1286–1292 (2008). doi:[10.1002/elan.200804226](https://doi.org/10.1002/elan.200804226)
224. F. Shang, J.D. Glennon, J.H.T. Luong, Glucose oxidase entrapment in an electropolymerized poly(tyramine) film with sulfobutylether- β -cyclodextrin on platinum nanoparticle modified boron-doped diamond electrode. *J. Phys. Chem. C* **112**(51), 20258–20263 (2008). doi:[10.1021/jp807482a](https://doi.org/10.1021/jp807482a)